

A Full Year Evaluation of the CALIOPE-EU Air Quality Modeling System over Europe for 2004

M. T. Pay^a, M. Piot^a, O. Jorba^a, S. Gassó^{a,b}, M. Gonçalves^{a,b}, S. Basart^a, D. Dabdub^d, P. Jiménez-Guerrero^c, J. M. Baldasano^{a,b,*}

jose.baldasano@bsc.es

^a*Earth Sciences Department, Barcelona Supercomputing Center, Barcelona, Spain*

^b*Environmental Modelling Laboratory, Technical University of Catalonia, Barcelona, Spain*

^c*Now at: Department of Physics, University of Murcia, Murcia, Spain*

^d*Department of Mechanical and Aerospace Engineering, University of California, Irvine, California, USA*

Abstract

The CALIOPE-EU high-resolution air quality modeling system, namely WRF-ARW/HERMES-EMEP/CMAQ/BSC-DREAM8b, is developed and applied to Europe (12 km × 12 km, 1hr). The model performances are tested in terms of air quality levels and dynamics reproducibility on a yearly basis. The present work describes a quantitative evaluation of gas phase species (O₃, NO₂ and SO₂) and particulate matter (PM_{2.5} and PM₁₀) against ground-based measurements from the EMEP (European Monitoring and Evaluation Programme) network for the year 2004. The evaluation is based on statistics. Simulated O₃ achieves satisfactory performances for both daily mean and daily maximum concentrations, especially in summer, with annual mean correlations of 0.66 and 0.69, respectively. Mean normalized errors are comprised within the recommendations proposed by the United States Environmental Protection Agency (US-EPA). The general trends and daily variations of primary pollutants (NO₂ and SO₂) are satisfactory. Daily mean concentrations of NO₂ correlate well with observations (annual correlation r=0.67) but tend to be underestimated. For SO₂, mean concentrations are well simulated (mean bias=0.5 μg m⁻³) with relatively high annual mean correlation (r=0.60), although peaks are generally overestimated. The dynamics of PM_{2.5} and PM₁₀ is well reproduced (0.49 < r < 0.62), but mean concentrations

*Corresponding author. Tel.: +34 93 413 77 19; fax: +34 93 413 77 21
Email address: *jose.baldasano@bsc.es* (J. M. Baldasano)

remain systematically underestimated. Deficiencies in particulate matter source characterization are discussed. Also, the spatially distributed statistics and the general patterns for each pollutant over Europe are examined. The model performances are compared with other European studies. While O₃ statistics generally remain lower than those obtained by the other considered studies, statistics for NO₂, SO₂, PM_{2.5} and PM₁₀ present higher scores than most models.

Keywords: Air quality, Model evaluation, Europe, High resolution, Ozone, Particulate matter

1 Introduction

Atmospheric pollutants have significant impact on many main fields. One of the major areas impacted is human health. High correlations between long-term exposure to fine particles and human health issues have been detected in population-based studies for several decades (Lave and Seskin, 1970; Thibodeau et al., 1980; Lipfert, 1994; Pénard-Morand et al., 2005). The latest studies even quantify the effects of aerosols on human lifespan. It is suggested that a decrease of 10 $\mu\text{g m}^{-3}$ in the concentration of fine particles may lead to an increase in life expectancy of 0.61 years (Pope et al., 2009). Another major area impacted by atmospheric pollutants is climate change. Particles scatter and absorb solar and infrared radiation in the atmosphere. In addition, they alter the formation and precipitation efficiency of liquid-water, ice and mixed-phase clouds (Ramanathan et al., 2001). Radiative forcing associated with these perturbations affects climate (Chylek and Wong, 1995; Jacobson, 2001). A third area impacted by air quality pollutants is atmospheric visibility. Since the size of atmospheric aerosols is similar to the wavelength of visible light, light is scattered and absorbed as it travels through the atmosphere (Japar et al., 1986; Adams et al., 1990). In brief, atmospheric pollutants are part of a highly complex system that affects the physics, chemistry, and life on the planet.

The European Commission (EC) and the US-EPA, among others, have shown great interest in the transport and dynamics of pollutants in the atmosphere. According to the European directives (European Commission, 1996, 2008), air quality modeling is a useful tool to understand the dynamics of air pollutants, to analyze and forecast the air quality, and to develop plans reducing emissions and alert the population when health-related issues occur. Both have set ambient air quality standards for acceptable levels of O₃ (European Commission, 2002), NO₂ and SO₂ (European Commission, 1999, 2001), PM_{2.5} and PM₁₀ in ambient air

28 (European Commission, 1999, 2001, 2008).

29 The CALIOPE project, funded by the Spanish Ministry of the Environment
30 and Rural and Marine Affairs (Ministerio de Medio Ambiente y Medio Rural
31 y Marino), has the main objective to establish an air quality forecasting system
32 for Spain (Baldasano et al., 2008b). In this framework, a high-resolution air
33 quality forecasting system, namely WRF-ARW/HERMES-EMEP/CMAQ/BSC-
34 DREAM8b, has been developed and applied to Europe (12 km \times 12 km, 1hr) as
35 well as to Spain (4 km \times 4 km, 1hr). The simulation of such a high-resolution
36 model system has been made possible by its implementation on the MareNostrum
37 supercomputer hosted by the Barcelona Supercomputing Center-Centro Nacional
38 de Supercomputaci3n (BSC-CNS). In order to reduce uncertainties, the model
39 system is evaluated with observational data to assess its capability of reproducing
40 air quality levels and the related dynamics.

41 A partnership of four Spanish research institutes composes the CALIOPE
42 project: the BSC-CNS, the “Centro de Investigaciones Energ3ticas, Medioambi-
43 entales y Tecnol3gicas” (CIEMAT), the Institute of Earth Sciences Jaume Almera
44 of the “Centro Superior de Investigaciones Cient3ficas” (IJA-CSIC) and the “Cen-
45 tro de Estudios Ambientales del Mediterraneo” (CEAM). This consortium deals
46 with both operational and scientific aspects related to air quality monitoring and
47 forecasting. BSC-CNS and CIEMAT lead the model developments of the project
48 while IJA-CSIC and CEAM are in charge of retrieving observational data for eval-
49 uation processes. Current experimental forecasts are available through
50 <http://www.bsc.es/caliope>.

51 Several operational air quality forecasting systems already exist in Europe
52 (see <http://gems.ecmwf.int> or <http://www.chemicalweather.eu>, Hewitt and Griggs,
53 2004; COST, 2009). CALIOPE advances our understanding of atmospheric dy-
54 namics in Europe as follows. First, CALIOPE includes a high-resolution compu-
55 tational grid. Most models use a horizontal cell resolution of at least 25 km \times
56 25 km for domains covering continental Europe. CALIOPE uses a 12 km \times 12
57 km cell resolution to simulate the European domain. Second, CALIOPE includes
58 a complex description of the processes involved in the modeling of particulate
59 matter. Both are important factors to obtain accurate results of air pollutant con-
60 centrations in a complex region such as southern Europe (Jim3nez et al., 2006).
61 Moreover, to date, none of the existing European operational systems include the
62 influence of Saharan dust on a non-climatic basis. Dust peaks cannot be repre-
63 sented by introducing boundary conditions derived from dust climatological data
64 due to the highly episodic nature of the events in the region (1- to 4-day average
65 duration) (Jim3nez-Guerrero et al., 2008). When considering only anthropogenic

66 emissions, chemical transport model simulations underestimate the PM10 con-
67 centrations by 30-50%, using the current knowledge about aerosol physics and
68 chemistry (Vautard et al., 2005a).

69 The purpose of the present paper is to provide a quantitative assessment of
70 the capabilities of the WRF-ARW/HERMES-EMEP/CMAQ/BSC-DREAM8b air
71 quality modeling system to simulate background concentrations of gas and par-
72 ticulate phase in the European domain. In the rest of the paper, this model sys-
73 tem will be named “CALIOPE-EU”. This evaluation intends to warrant the use
74 of such simulation for further nested calculations on the smaller domain of the
75 Iberian Peninsula (principal goal of the CALIOPE project). The results are eval-
76 uated statistically and dynamically, compared to performance goals and criteria,
77 and to other model performances.

78 In this paper, Sect. 2 describes the models, the observational dataset and the
79 statistical parameters calculated. Section 3 analyses the model results against
80 available measurement data for the year 2004 and the modeled annual distribu-
81 tion of O₃, NO₂, SO₂, PM2.5 and PM10. A thorough comparison with other
82 European studies is presented in Sect. 4. Conclusions are drawn in Sect. 5.

83 2. Methods

84 2.1. Model Description

85 CALIOPE is a state-of-the-art modeling framework currently under further de-
86 velopment. As shown in Fig. 1, CALIOPE-EU is a complex system that integrates
87 a meteorological model (WRF-ARW), an emission processing model (HERMES-
88 EMEP), a mineral dust dynamic model (BSC-DREAM8b), and a chemical trans-
89 port model (CMAQ) together in an air quality model system.

90 2.1.1. Meteorology

91 The Advanced Research Weather Research and Forecasting (WRF-ARW) Model
92 v3.0.1.1 (Michalakes et al., 2004; Skamarock and Klemp, 2008) is used to provide
93 the meteorology to the chemical transport model. WRF is a fully compressible,
94 Eulerian non-hydrostatic model that solves the equations that govern the atmo-
95 spheric motions. Microphysical processes are treated using the single-moment
96 3-class scheme as described in Hong et al. (2004). The sub-grid-scale effects of
97 convective and shallow clouds are resolved by a modified version of the Kain-
98 Fritsch scheme based on Kain and Fritsch (1990) and Kain and Fritsch (1993).
99 The surface layer scheme uses stability functions from Paulson (1970), Dyer and
100 Hicks (1970), and Webb (1970) to compute surface exchange coefficients for heat,

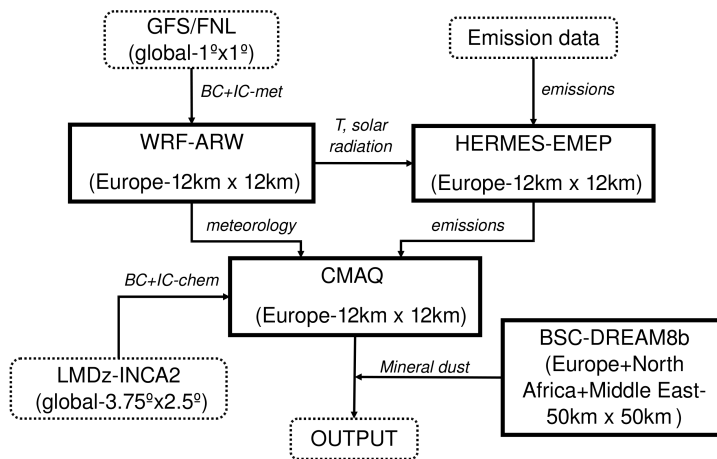


Figure 1: Modular structure of the CALIOPE-EU modeling system used to simulate air quality dynamics in Europe. Squared boxes with solid lines represent the main models of the framework. Boxes with dashed lines represent input/output dataset. Lines connecting boxes represent the information flow.

101 moisture, and momentum. The Noah Land-Surface scheme is used to provide heat
 102 and moisture fluxes over land points and sea-ice points. It is a 4-layer soil tem-
 103 perature and moisture model with canopy and snow cover prediction. The vertical
 104 sub-grid-scale fluxes caused by eddy transport in the atmospheric column are re-
 105 solved by the Yonsei University planetary boundary layer (PBL) scheme (Noh
 106 et al., 2003). Finally, long-wave radiative processes are parameterized with the
 107 Rapid Radiative Transfer Model (Mlawer et al., 1997) while the short-wave radia-
 108 tive scheme is based on Dudhia (1989).

109 2.1.2. Emissions

110 The emission model is the High-Selective Resolution Modelling Emission Sys-
 111 tem (HERMES, see Baldasano et al., 2008a). HERMES uses information and
 112 state-of-the-art methodologies for emission estimations. It calculates emissions
 113 by sector-specific sources or by individual installations and stacks. Raw emission
 114 data are processed by HERMES in order to provide a comprehensive description
 115 of the emissions to the air quality model. Emissions used for the European do-
 116 main are derived from the 2004 annual EMEP emission database (EMEP, 2007).
 117 Disaggregation of EMEP (50 km resolution) data is performed in space (12 km
 118 \times 12 km) and time (1h). The spatial and temporal top-down disaggregation is

119 sector-dependent. A Geographical Information System (GIS) is used to remap
120 the data to the finer grid applying different criteria through three datasets: a high-
121 resolution land use map (EEA, 2000), coordinates of industrial sites (European
122 Pollutant Emission Register (EPER), Pulles et al., 2006), and vectorized road car-
123 tography of Europe (ESRI, 2003). In the vertical dimension, the sector dependent
124 emission distribution for gases is applied following the EMEP model (widely used
125 for regional air quality studies in Europe, Simpson et al., 2003). Distinct distri-
126 butions are used for aerosols, leading in most cases to lower average emission
127 heights than for gas phase emissions (De Meij et al., 2006; Pregger and Friedrich,
128 2009). In the time dimension, data are mapped from annual resolution to an hourly
129 basis using the temporal factors of EMEP/MSC-W (Meteorological Synthesizing
130 Centre-West).

131 2.1.3. Chemistry

132 The selected chemical transport model is the Models-3 Community Multi-
133 scale Air Quality Modeling System (Models-3/CMAQ, Byun and Ching, 1999;
134 Binkowski, 1999; Byun and Schere, 2006). CMAQ is used to study the behavior of
135 air pollutants from regional to local scales due to its generalized coordinate system
136 and its advanced nesting grid capability. CMAQ version 4.5, used in this study,
137 has been extensively evaluated under various conditions and locations (Wyat Ap-
138 pel et al., 2007, 2008; Roy et al., 2007). Following the criteria of Jiménez et al.
139 (2003) the Carbon Bond IV chemical mechanism is applied (CBM-IV, Gery et al.,
140 1989). It includes aerosol and heterogeneous chemistry. The production of sea
141 salt aerosol (SSA) is implemented as a function of wind speed and relative hu-
142 midity (Gong, 2003; Zhang et al., 2005) through the AERO4 aerosol module.
143 The AERO4 module distinguishes among different chemical aerosol components
144 namely nitrate, sulfate, ammonium, elemental carbon, organic carbon with three
145 subcomponents (primary, secondary anthropogenic and secondary biogenic), soil,
146 sodium, and chlorine. Unspecified anthropogenic aerosols and aerosol water are
147 additionally kept as separate components. Aerosols are represented by three size
148 modes (Aitken, accumulation and coarse mode), each of them assumed to have
149 a lognormal distribution (Binkowski and Roselle, 2003). Secondary inorganic
150 aerosols (SIA) are generated by nucleation processes from their precursors to form
151 nitrate ammonium and sulfate aerosols. Secondary organic aerosol (SOA) can be
152 formed from aromatics (anthropogenic organic aerosols) and terpenes (biogenic
153 organic aerosols, Schell et al., 2001). The aerosol microphysical description is
154 based on a modal aerosol model (Binkowski and Roselle, 2003) using the ISOR-
155 ROPIA thermodynamic equilibrium model (Nenes et al., 1998). For a more com-

156 plete description of the processes implemented in CMAQ, the reader is referred to
157 Byun and Schere (2006).

158 2.1.4. Mineral Dust

159 The Dust REgional Atmospheric Model (BSC-DREAM8b) was designed to
160 simulate and/or predict the atmospheric cycle of mineral dust (Nickovic et al.,
161 2001; Pérez et al., 2006a,b). The simulations cover the Euro-Mediterranean and
162 East-Asia areas. The aerosol description was improved from 4 to 8 bins to al-
163 low a finer description of dust aerosols. In this version dust-radiation interactions
164 are included. The partial differential nonlinear equation for dust mass continuity
165 is resolved in the Eulerian mode. BSC-DREAM8b is forced by the NCEP/Eta
166 meteorological driver (Janjic, 1977, 1979, 1984, 1990, 1994). BSC-DREAM8b
167 simulates the long-range transport of mineral dust at a $50 \text{ km} \times 50 \text{ km}$ resolution
168 using 24 vertical layers extending up to 15 km, every one hour. In this version
169 dust-radiation interactions are included. An offline coupling is applied to the cal-
170 culated concentrations of particulate matter from CMAQ (Jiménez-Guerrero et al.,
171 2008).

172 2.2. Model Setup

173 The model system is initially run on a regional scale ($12 \text{ km} \times 12 \text{ km}$ in space
174 and 1 hour in time) to model the European domain. WRF is configured with a
175 grid of 479×399 points and 38 σ vertical levels (11 characterizing the PBL). The
176 model top is defined at 50 hPa to resolve properly the troposphere-stratosphere
177 exchanges.

178 The simulation consists of 366 daily runs to simulate the entire year of 2004.
179 The choice for this specific year is based on the direct availability of the HERMES-
180 EMEP emission model for this year. The first 12 hours of each meteorological run
181 are treated as cold start, and the next 23 hours are provided to the chemical trans-
182 port model. The Final Analyses of the National Centers of Environmental Predic-
183 tion (FNL/NCEP) at 12 hours UTC are used as initial conditions. The boundary
184 conditions are provided at intervals of 6 hours. The FNL/NCEP data have a spatial
185 resolution of $1^\circ \times 1^\circ$.

186 The CMAQ horizontal grid resolution corresponds to that of WRF. Its vertical
187 structure was obtained by a collapse from the 38 WRF layers to a total of 15 layers
188 steadily increasing from the surface up to 50 hPa with a stronger concentration
189 within the PBL.

190 Due to uncertain external influence, the definition of adequate lateral bound-
191 ary conditions for gas phase chemistry in a regional model is a complex issue and

192 an important source of errors. Variable intercontinental transport of pollutants
193 substantially influences the levels of pollution in Europe (see, e.g., Li et al., 2002;
194 Guerova et al., 2006). This air quality issue has been extensively studied. Re-
195 cent works addressed the use of global chemical models to investigate the impact
196 of chemical boundary conditions on regional scale O₃ concentrations. Various
197 studies were performed over the U.S. (Tang et al., 2007, 2008; Song et al., 2008;
198 Reidmiller et al., 2009), whereas investigations over Europe remain scarce (Szopa
199 et al., 2009). In a previous assessment of the model performances of CALIOPE-
200 EU (Jiménez-Guerrero et al., 2008), static chemical boundary conditions, adapted
201 from Byun and Ching (1999), were used. In the present work, boundary con-
202 ditions are based on the global climate chemistry model LMDz-INCA2 (96 ×
203 72 grid cells, namely 3.75° × 2.5° in longitude and latitude, with 19 σ -p hybrid
204 vertical levels, Szopa et al., 2009) developed by the Laboratoire des Sciences du
205 Climat et l'Environnement (LSCE). Monthly mean data for the year 2004 are in-
206 terpolated in the horizontal and vertical dimensions to force the major chemical
207 concentrations at the boundaries of the domain (Piot et al., 2008). A detailed de-
208 scription of the INteractive Chemistry and Aerosol (INCA) model is presented in
209 Hauglustaine et al. (2004) and Folberth et al. (2006).

210 2.3. Air Quality Network

211 Model output for gas and particulate phase concentrations are compared with
212 ground-based measurements from the EMEP monitoring network for the year
213 2004. According to the criteria proposed by the European Environment Agency
214 (EEA, Larssen et al., 1999), EMEP stations are located at a minimum distance
215 of approximately 10 km from large emission sources. Consequently, all EMEP
216 stations are assumed to be representative of regional background concentrations
217 (Torseth and Hov, 2003). Therefore, the authors wish to stress that the model per-
218 formances presented in this paper are evaluated only for background concentra-
219 tions. The measurements are well documented and freely available on the EMEP
220 web page (<http://www.emep.int>).

221 Before comparing the model results with EMEP data, the available measure-
222 ments were filtered, and uncertain data (before and after a measurement interrup-
223 tion or a calibration of equipment) were removed. After this filtering, only obser-
224 vational sites with a temporal coverage greater than 85% were selected. Note that
225 the final coverage of the dataset is rather disperse where France, Italy and south-
226 eastern Europe only include several stations. Measurement data used in this paper
227 are given on a daily average. As a result, 60 stations were selected to evaluate
228 O₃, 43 for NO₂, 31 for SO₂, 16 for PM_{2.5} and 25 for PM₁₀, respectively. The

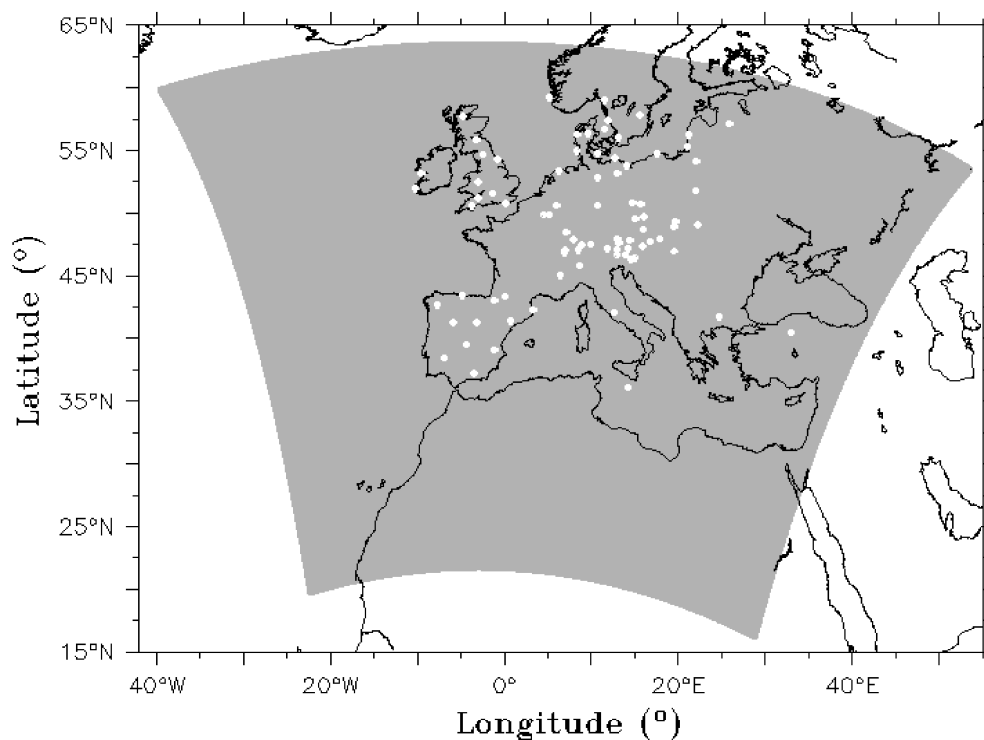


Figure 2: Grey shaded area: modeling domain used in this study. The white filled circles represent the selected subset of EMEP data collection sites. Characteristics of each station are listed in Table 1.

229 selected EMEP stations and measured pollutants that are used for this comparison
230 are briefly described in Table 1 and their locations are displayed in Fig. 2.

231 As EMEP aerosol measurements supposedly remove all water content from
232 samples to consider only dry aerosols, the simulated aerosol water was not taken
233 into account in the model-to-data comparisons. However, as noted by Tsyro
234 (2005), residual water persisting in sampled aerosols from EMEP may induce
235 a substantial underprediction by the simulated dry aerosol concentrations. More-
236 over, although the aerodynamic diameter is used for PM₁₀ and PM_{2.5} in measure-
237 ment techniques, the model only considers the Stokes diameter to characterize the
238 aerosol geometry. For more details on this issue, see Jiang et al. (2006).

Table 1: Location and characteristics of selected EMEP stations for 2004 on a daily basis.

	Station code ^a	Latitude ^b	Longitude ^b	Altitude (m)	Station name	O ₃	NO ₂	SO ₂	Total PM10	Total PM2.5
1	AT02	+47.767	+16.767	117	Illmitz	x ^c	x	x ^c	x	x
2	AT04	+47.650	+13.200	851	St. Koloman			x		
3	AT05	+46.678	+12.972	1020	Vorhegg	x ^c				x
4	AT30	+48.721	+15.942	315	Pillersdorf bei Retz	x ^c				
5	AT32	+47.529	+9.927	1020	Sulzberg	x ^c				
6	AT33	+47.129	+14.204	1302	Stolzalpe bei Murau	x ^c				
7	AT34	+47.054	+12.958	3106	Sonnblick	x ^c				
8	AT37	+47.137	+11.870	1970	Zillertaler Alpen	x ^c				
9	AT38	+46.694	+13.915	1895	Gerlitzten	x ^c				
10	AT40	+47.348	+15.882	1170	Masenberg	x ^c				
11	AT41	+47.973	+13.016	730	Haunsberg	x ^c				
12	AT48	+47.833	+14.433	899	Zoebelboden	x ^c				
13	BG53	+41.700	+24.733	1750	Rojen peak	x ^c				
14	CH02	+46.817	+6.950	510	Payerne		x	x	x	x
15	CH03	+47.483	+8.900	540	Tänikon		x			x
16	CH04	+47.051	+6.981	1130	Chaumont	x ^c	x	x	x	x
17	CH05	+47.069	+8.466	1030	Rigi	x ^c	x	x		x
18	CZ01	+49.733	+16.033	737	Svratouch	x ^c	x	x		
19	CZ03	+49.583	+15.083	534	Kosetice	x ^c	x	x		
20	DE01	+54.926	+8.310	12	Westerland					x
21	DE02	+52.800	+10.750	74	Langenbrgge		x	x	x	x
22	DE03	+47.915	+7.909	1205	Schauinsland	x ^c			x	x
23	DE07	+53.167	+13.033	62	Neuglobsow					x
24	DE08	+50.650	+10.767	937	Schmücke					x
25	DE09	+54.433	+12.733	1	Zingst	x ^c				x
26	DE26	+53.750	+14.067	1	Ueckermünde	x ^c				
27	DE35	+50.833	+14.767	490	Lückendorf	x ^c				
28	DK03	+56.350	+9.600	13	Tange			x		
29	DK05	+54.733	+10.733	10	Keldsnor					x
30	DK08	+56.717	+11.517	40	Anholt		x	x		
31	DK31	+56.283	+8.433	10	Ulborg	x ^c				
32	ES07	+37.233	-3.533	1265	Víznar	x ^c	x ^c		x	x
33	ES08	+43.442	-4.850	134	Niembro	x ^c	x ^c	x ^c	x	x
34	ES09	+41.281	-3.143	1360	Campisábalos	x ^c	x ^c	x ^c	x	x
35	ES10	+42.319	+3.317	23	Cabo de Creus	x ^c	x ^c		x	x
36	ES11	+38.476	-6.923	393	Barcarrota		x ^c	x ^c	x	x
37	ES12	+39.086	-1.102	885	Zarra	x ^c	x ^c	x ^c	x	x
38	ES13	+41.283	-5.867	985	Penausende	x ^c	x ^c	x ^c	x	x
39	ES14	+41.400	+0.717	470	Els Torms	x ^c	x ^c	x ^c	x	x
40	ES15	+39.517	-4.350	1241	Risco Llano	x ^c	x ^c	x ^c	x	x
41	ES16	+42.653	-7.705	506	O Saviñao	x ^c	x ^c	x ^c	x	x
42	FR08	+48.500	+7.133	775	Donon	x ^c	x ^c	x		
43	FR09	+49.900	+4.633	390	Revin	x ^c		x		
44	FR12	+43.033	-1.083	1300	Iraty	x ^c		x		
45	FR13	+43.375	+0.104	236	Peyrusse Vieille	x ^c	x ^c	x		
46	FR16	+45.000	+6.467	746	Le Casset	x ^c				
47	GB13	+50.596	-3.713	119	Yarner Wood	x ^c				
48	GB14	+54.334	-0.808	267	High Muffles	x ^c				
49	GB15	+57.734	-4.774	270	Strath Vaich Dam	x ^c				
50	GB31	+52.504	-3.033	370	Aston Hill	x ^c				
51	GB33	+55.859	-3.205	180	Bush	x ^c				
52	GB35	+54.684	-2.435	847	Great Dun Fell	x ^c				
53	GB36	+51.573	-1.317	137	Harwell	x ^c	x ^c			
54	GB37	+53.399	-1.753	420	Ladybower Res.	x ^c	x ^c			

Table 2: Continued.

Station code ^a	Latitude ^b	Longitude ^b	Altitude (m)	Station name	O ₃	NO ₂	SO ₂	Total PM10	Total PM2.5
55 GB38	+50.793	+0.179	120	Lullington Heath	x ^c	x ^c			
56 GB44	+51.231	-3.048	55	Somerton	x ^c				
57 HU02	+46.967	19.583	125	K-pusza		x			
58 IE01	+51.940	-10.244	11	Valentina Observatory	x ^c	x			
59 IE31	+53.167	-9.500	15	Mace Head	x ^c				
60 IT01	+42.100	+12.633	48	Montelibretti		x	x		x
61 IT04	+45.800	+8.633	209	Ispra		x		x	x
62 LT15	+55.350	+21.067	5	Preilla	x ^c	x	x		
63 LV10	+56.217	+21.217	5	Rucava	x ^c	x	x		
64 LV16	+57.133	+25.917	183	Zoseni		x	x		
65 NL09	+53.334	+6.277	1	Kullumerwaard		x ^c			
66 MT01	+36.100	+14.200	160	Giordan lighthouse	x ^c				
67 NO43	+59.000	+11.533	160	Prestebakke	x ^c				
68 NO52	+59.200	+5.200	15	Sandve	x ^c				
69 PL02	+51.817	+21.983	180	Jarczew	x ^c	x	x		
70 PL03	+50.733	+15.733	1603	Sniezka	x ^c	x	x		
71 PL04	+54.750	+17.533	2	Leba	x ^c	x	x		
72 PL05	+54.150	+22.067	157	Diabla Gora		x			
73 SE11	+56.017	+13.150	175	Vavihill	x ^c	x	x		
74 SE14	+57.400	+11.917	5	Råö	x ^c	x			
75 SE32	+57.817	+15.567	261	Norra-Kvill	x ^c				
76 SI31	+46.429	+15.003	770	Zarodnje	x ^c				
77 SI32	+46.299	+14.539	1740	Krvavec	x ^c				
78 SK02	+48.933	+19.583	2008	Chopok		x			
79 SK05	+49.367	+19.683	892	Liesek		x			
80 SK06	+49.050	+22.267	345	Starina		x	x		
81 SK07	+47.960	+17.861	113	Topolniky		x			
82 TR01	+40.500	+33.000	1169	Cubuk II		x			

^a 2-letter country code plus 2-digit station code.

^b A positive value indicates northern latitudes or eastern longitudes. A negative value indicates southern latitudes or western longitudes.

^c Daily concentration calculated from hourly data.

239 2.4. Statistical Indicators

240 There are a number of metrics that can be used to examine performances of
241 air quality models (U.S. EPA, 1984, 1991; Cox and Tikvart, 1990; Weil et al.,
242 1992; Chang and Hanna, 2004; Boylan and Russell, 2006). In particular, mean
243 normalized bias error (MNBE) and mean normalized gross error (MNGE) nor-
244 malizing the bias and error for each model-observed pair by the observation are
245 useful parameters. Correlation coefficient (r), root mean square errors (RMSE)
246 and mean bias (MB) values are also commonly used by the modeling community.
247 For the evaluation of particulate matter concentrations, Boylan and Russell (2006)
248 indicated that MNBE and MNGE may not be appropriate and suggested the mean
249 fractional bias (MFB) and the mean fractional error (MFE) parameters instead.

250 The US-EPA suggested several performance criteria for simulated O_3 , such
251 as $MNBE \leq \pm 15\%$ and $MNGE \leq 35\%$ (U.S. EPA, 1991, 2007) whereas the
252 EC proposes a maximum uncertainty between measured and modeled concentra-
253 tions of 50% and 30% for $O_3/NO_2/SO_2$ daily mean and NO_2/SO_2 annual mean,
254 respectively (European Commission, 2008). For particulate matter, Boylan and
255 Russell (2006) proposed that the model performance goal be met when both the
256 MFE and MFB are less than or equal to 50% and $\pm 30\%$, respectively, and the
257 model performance criterion be met when both $MFE \leq 75\%$ and $MFB \leq 60\%$.
258 All these criteria and goals are selected to provide metrics for the CALIOPE-EU
259 model performances.

260 The model-to-data statistics MB, RMSE, MNBE, MNGE, MFB and MFE are
261 selected for the present study, together with the measured and modeled mean and
262 the correlation coefficient. Annual and seasonal mean statistics are computed,
263 with seasons corresponding to winter (January, February and December), spring
264 (March, April and May), summer (June, July and August) and fall (September,
265 October and November).

266 It is important to note that, unless explicitly stated otherwise, the statistical
267 norms are calculated without any minimum threshold when considering the mea-
268 surement data. However, in the present work, statistics of annual means using
269 thresholds are also computed. In that case we chose $80 \mu\text{g m}^{-3}$ for O_3 (according
270 to recommendations of the US-EPA, U.S. EPA, 1991; Russell and Dennis, 2000),
271 $1.5 \mu\text{g m}^{-3}$ for NO_2 , $0.2 \mu\text{g m}^{-3}$ for SO_2 , $1.5 \mu\text{g m}^{-3}$ for PM_{10} and $3.5 \mu\text{g m}^{-3}$
272 for $PM_{2.5}$, respectively.

273 3. Results and Discussion

274 As CALIOPE-EU is a fundamental model system the authors wish to stress
275 that, apart from the discussion of the Fig. 6 and its related statistics (Table 4),
276 neither correction factors nor any adjusting model parameterization were applied
277 to the model output or the original model codes. First, in Sect. 3.1, a thorough
278 model evaluation is performed through statistical and dynamical performances.
279 Later, in Sect. 3.2, a general description of the annual mean distribution of each
280 pollutant is provided to determine each pattern throughout Europe.

281 3.1. Model evaluation

282 Fig. 3 represents (left) the temporal series of the model (black lines) and daily
283 measured EMEP data (grey lines) as an average of all the stations for each pol-
284 lutant over the complete year 2004, together with (right) the scatterplot of the
285 modeled-measured daily data. Table 3 shows annual and seasonal statistics cal-
286 culated at the location of all EMEP stations. Statistics are calculated for daily
287 averages of O_3 , NO_2 , SO_2 , $PM_{2.5}$ and PM_{10} . In the case of O_3 , the daily peak of
288 hourly mean O_3 is also computed as it is one of the most important parameters to
289 be considered.

290 3.1.1. Ozone

291 A total of 60 EMEP stations constitute the O_3 measurement dataset to be com-
292 pared to the simulation (see Table 1). In Fig. 3a, the time series of both simulated
293 and observed O_3 concentrations are presented. The annual trend is well captured
294 with an annual correlation of daily mean and daily peak concentrations of 0.66
295 and 0.69, respectively (see Table 3). Although the annual daily mean bias is null,
296 the inter-annual variability leads to an annual RMSE of up to $20.6 \mu g m^{-3}$. An-
297 nual and seasonal MNBE and MNGE values for daily mean and daily maximum
298 concentrations show relatively good performances which are in accordance with
299 the recommendations of the EC and the US-EPA (see Sect. 2.4).

300 Results show distinct inter-seasonal behaviors between colder and warmer
301 months. From January to March and from October to December, the model tends
302 to underestimate the mean concentrations (in winter, $MB = -5.8 \mu g m^{-3}$), while
303 it slightly overestimates concentrations in summer months ($MB = 7.5 \mu g m^{-3}$).
304 Correlation values are lowest for both daily mean and daily peak correlations in
305 the winter ($r = 0.54$ and 0.50 , respectively). This inter-seasonal variability is at-
306 tributed to the model sensitivity to boundary conditions near the surface in winter.
307 During decreases of photochemical reactions in fall and winter the concentrations

Table 3: Seasonal and annual statistics obtained with CALIOPE-EU over Europe for 2004 at the EMEP stations. Winter: January, February and December; Spring: March, April, May; Summer: June, July, August; Fall: September, October, November. The number of data points indicates the number of pair measurement-model used to compute the statistics. The calculated statistics are: measured mean for available data ($\mu\text{g m}^{-3}$), modeled mean for the whole year ($\mu\text{g m}^{-3}$), correlation (r), Mean Bias (MB, $\mu\text{g m}^{-3}$), Root Mean Square Error (RMSE, $\mu\text{g m}^{-3}$), Mean Normalized Bias Error (MNBE, %), Mean Normalized Gross Error (MNGE, %), Mean Fractional Bias (MFB, %) and Mean Fractional Error (MFE, %). For the annual mean calculated with threshold, we used $80 \mu\text{g m}^{-3}$ for O_3 , $1.5 \mu\text{g m}^{-3}$ for NO_2 , $0.2 \mu\text{g m}^{-3}$ for SO_2 , $1.5 \mu\text{g m}^{-3}$ for $\text{PM}_{2.5}$ and $3.5 \mu\text{g m}^{-3}$ for PM_{10} , respectively. Seasonal statistics are computed without threshold.

	Period	Data points	Measured mean	Modeled mean	r	MB	RMSE	MNBE	MNGE	MFB	MFE
O ₃ daily (60 stations)	Winter	5257	60.8	54.8	0.54	-5.8	21.4	-1	34	-11	32
	Spring	5466	84.5	82.6	0.55	-1.8	20.8	0	21	-4	22
	Summer	5443	79.5	86.9	0.64	7.5	19.8	15	23	11	20
	Fall	5197	60.7	60.1	0.58	-0.3	20.3	9	34	-1	30
	Annual (no threshold)	21363	71.6	71.2	0.66	0.0	20.6	6	28	-1	26
	Annual (threshold)	7299	96.9	91.1	0.44	-5.9	20.5	-6	17	-8	19
O ₃ daily peak (60 stations)	Winter	5257	73.7	67.3	0.50	-6.2	24.1	-5	28	-12	29
	Spring	5466	101.9	97.3	0.55	-4.5	21.5	-4	18	-6	19
	Summer	5443	101.1	100.5	0.65	-0.5	20.2	3	16	1	16
	Fall	5197	77.2	70.2	0.65	-6.6	21.2	-6	25	-11	26
	Annual (no threshold)	21363	88.7	83.9	0.69	-4.4	21.8	-3	22	-7	22
	Annual (threshold)	12891	104.2	97.5	0.54	-6.7	22.4	-6	18	-9	19
NO ₂ daily (43 stations)	Winter	3600	12.1	8.0	0.67	-4.2	12.7	3	57	-21	55
	Spring	3787	9.4	4.8	0.66	-4.5	10.6	-27	53	-51	67
	Summer	3843	6.2	3.5	0.59	-2.7	5.7	-29	54	-53	69
	Fall	3725	9.4	6.0	0.66	-3.4	10.1	-15	48	-34	56
	Annual (no threshold)	15035	9.3	5.6	0.67	-3.7	10.1	-17	53	-40	62
	Annual (threshold)	14138	9.8	5.8	0.66	-4.0	10.4	-20	51	-42	61
SO ₂ daily (31 stations)	Winter	2629	2.2	2.6	0.62	0.5	2.9	80	122	8	70
	Spring	2749	1.6	2.0	0.63	0.4	1.9	62	96	13	62
	Summer	2707	1.2	1.6	0.49	0.4	1.8	86	121	14	65
	Fall	2604	1.4	2.0	0.56	0.7	2.3	105	134	25	68
	Annual (no threshold)	10689	1.6	2.1	0.60	0.5	2.2	83	118	15	66
	Annual (threshold)	10384	1.7	2.2	0.60	0.5	2.3	72	108	13	65
PM _{2.5} daily (16 stations)	Winter	1171	13.7	4.8	0.62	-8.4	15.3	-47	59	-78	86
	Spring	1264	12.2	5.2	0.50	-6.7	10.6	-50	59	-79	84
	Summer	1396	12.2	6.8	0.49	-5.4	9.1	-45	56	-71	78
	Fall	1287	11.5	6.2	0.52	-5.0	9.3	-39	53	-62	72
	Annual (no threshold)	5118	12.3	5.7	0.47	-6.3	11.2	-45	56	-72	80
	Annual (threshold)	4756	13.0	6.3	0.45	-6.7	11.6	-46	57	-74	81
PM ₁₀ daily (25 stations)	Winter	1994	18.0	6.6	0.54	-11.2	18.2	-47	60	-78	86
	Spring	2087	17.7	7.1	0.54	-10.5	15.0	-54	59	-84	87
	Summer	2204	18.5	8.2	0.60	-10.5	16.1	-54	58	-83	86
	Fall	2104	17.0	8.1	0.62	-9.0	13.5	-44	55	-70	77
	Annual (no threshold)	8389	17.8	7.5	0.57	-10.3	15.8	-50	58	-79	84
	Annual (threshold)	7918	18.7	7.8	0.55	-10.9	16.2	-53	57	-82	85

308 defined at the boundaries proportionally acquire an increasing role in the control
309 of the concentration levels simulated within the domain. Also, the large concentra-
310 tions of O_3 in the highest layers of the boundary profile (reaching the stratosphere)
311 was found to be responsible for episodic inaccurate stratosphere-troposphere ex-
312 changes during colder months (not shown here; also see Eisele et al., 1999; Cristo-
313 fanelli and Bonasoni, 2009). Such finding was highlighted very recently by Lam
314 and Fu (2009) who pointed the inaccurate treatment of the tropopause in CMAQ
315 as the issue causing such artifact. On the other hand, the mean biases for daily and
316 daily peak concentrations are positive during warmer months with lowest RMSE
317 values (19.8 and 20.2 $\mu g m^{-3}$ in summer, respectively). Model-observations cor-
318 relations, MNBE and MNGE values also reach the best values during this period.
319 This performance demonstrates the greater ability of the model to accurately simu-
320 late ozone during its intense photochemical formation in warmer months. Daily
321 variations are satisfactorily reproduced (see scatter plot in Fig. 3b with nearly 95%
322 of the data points falling within the 1:2 and 2:1 factor range). However, due to un-
323 certainties in the modeled nocturnal NO_x cycle, the O_3 chemistry at night tends to
324 overpredict the observed concentrations. Such behaviour is partly reflected by the
325 difference between the annual mean biases calculated with or without the mini-
326 mum threshold of 80 $\mu g m^{-3}$ on the measured data. By implementing this thresh-
327 old a part of overestimated nocturnal measured values is not considered which
328 induces a negative value of -5.9 $\mu g m^{-3}$ compared to 0.0 using no threshold. For
329 extreme values (above 150 $\mu g m^{-3}$) the observed concentrations are systemati-
330 cally underestimated by the model (see Fig. 3b). This behavior is most likely
331 caused by high local pollution transported to rural sites but not captured with the
332 current horizontal resolution of the model (see Ching et al., 2006).

333 Fig. 4 and Fig. 5 present the spatial distributions in winter (left) and summer
334 (right) of the correlation and mean bias, respectively, without threshold on mea-
335 surements. In the case of O_3 two different spatial regimes can be distinguished:
336 seasonal correlations are highest in England, central and southern Europe, while
337 Ireland and the countries along the North and Baltic Seas present lower perfor-
338 mances. We attribute these lower performances of the model at these locations
339 mostly to their relative proximity with the northern boundary of the domain. The
340 most remote sites with low levels of O_3 display the lowest seasonal correlations
341 (see Irish and northern stations; from -0.2 to 0.2 in winter, from 0 to 0.4 in sum-
342 mer). The model skills improve notably from winter to summer as a result of the
343 increasing importance of the photochemical production of ozone. In summer most
344 of the seasonal correlations are comprised between 0.4 and 0.9. Also, statistics are
345 surprisingly satisfactory in complex regions such as the Alpine (stations CH02 to

346 CH05 and FR16) or the Pyrenean chains (FR12). As mentioned above in this
347 section the model tends to underestimate the mean concentrations in winter and
348 overestimate in summer (Fig. 5). It is noted that mean biases in southern Europe
349 have an inter-seasonal variability less pronounced than in the rest of Europe with
350 values rather positive. In summer, the lowest MB values are found in regions of
351 low mean O_3 levels such as the Alpine chain, Ireland and some Spanish stations.

352 3.1.2. Nitrogen Dioxide

353 As shown in Table 1, 43 stations were used to provide NO_2 measurements
354 throughout Europe. The temporal and spatial variability of the simulated NO_2
355 in Europe is larger than for O_3 , reflecting its higher sensitivity to meteorology
356 and model resolution (Vautard et al., 2009). The model-observations comparison,
357 presented in Fig. 3c and Fig. 3d highlights a correct annual trend, but with a sys-
358 tematic negative bias throughout the year. The dynamics is often well captured
359 but the amplitude of daily variations is underestimated. These low variations have
360 a direct impact on the daily variations of ozone in the PBL.

361 The annual average correlation is high ($r=0.67$, see Table 3), with better per-
362 formances in winter than in summer. Chemical processes, less dominant com-
363 pared to transport in winter, could explain such differences (Bessagnet et al.,
364 2004). Annual and seasonal mean biases are relatively high, ranging from -4.5
365 to $-2.7 \mu g m^{-3}$, leading to mean normalized error values rather near the maxi-
366 mum uncertainty proposed by the EC. High measured concentrations (above 70
367 $\mu g m^{-3}$) are particularly underestimated (see Fig. 3d). When comparing modeled
368 results versus measured data, 59.1% of the corresponding data pairs fall within a
369 factor of 2 of each other, and 92.9% within a factor of 5.

370 The statistics of the model are spatially displayed in Fig. 4 and Fig. 5. NO_2
371 concentrations are mostly driven by local to regional emissions. Therefore, re-
372 mote and clean boundary conditions are not significant contributors to the sim-
373 ulated concentrations of NO_2 in Europe. Correlations are highest in winter for
374 the areas including UK, northern countries and some spanish stations. In these re-
375 gions emissions of NO_x are generally either high or very low (also see Sect. 3.2.2).
376 Low correlations are mainly concentrated in central Europe (coefficients between
377 -0.2 and 0.4). Numerous stations located in low- NO_2 areas display satisfactory
378 seasonal mean biases (see northern and central Europe and Spain with seasonal
379 $MB = \pm 2 \mu g m^{-3}$), while stations substantially affected by transport from source
380 regions display the highest seasonal mean biases (Fig. 5). The aforementioned
381 large underestimations of high measured concentrations are mainly caused by the
382 three stations from Great Britain (GB36, GB37 and GB38, see Table 1). These

383 stations frequently undergo high pollution events caused by emissions from road
384 traffic and combustion processes. To a lesser extent, these highly polluted plumes
385 from the United Kingdom (UK) also affect the measuring station in The Nether-
386 lands (NL09) under westerly winds and contribute to the increase in mean bias
387 values when the transport is not accurately simulated. At these locations, negative
388 mean biases reaching up to $22 \mu\text{g m}^{-3}$ on annual average are noted with highest
389 biases in winter. Such differences are most likely caused by the underestimation
390 of emission sources in these areas. Altogether, the analysis of the spatial distri-
391 bution of the model skills shows that the level NO_2 concentrations at very rural
392 stations is well captured but with low correlation coefficients, while mean biases
393 and correlation coefficients are greatest at polluted stations.

394 Apart from sources unaccounted for in the emission database, uncertainties
395 may also arise in the spatial and temporal distribution of the sources (Stern et al.,
396 2008). In the PBL NO_x concentrations are dominated by emissions near the sur-
397 face, such as traffic and domestic heating, which are subject to strong spatial and
398 temporal variations.

399 3.1.3. Sulfur Dioxide

400 For SO_2 , the model results were evaluated against 31 EMEP stations mea-
401 suring daily mean concentrations of SO_2 at background sites. The stations are
402 located across the Iberian Peninsula, central and north-eastern Europe. It is worth
403 noting that the daily mean concentrations are low and provide information about
404 the background levels of SO_2 across Europe only. Fig. 3e shows the time series
405 of the daily mean concentrations of SO_2 at the EMEP stations together with the
406 model simulation at these stations. Results show that SO_2 concentrations are well
407 captured by the model, although some observed peaks are overestimated. During
408 the cold months (January, February, March, October, November) the model agrees
409 well with observations, and monthly variations of SO_2 are well captured. On the
410 other hand, during the warm period (April, May, June, July, August and Septem-
411 ber) results present an overall positive bias of $1 \mu\text{g m}^{-3}$. September and December
412 months are characterized by some episodes of large overestimations. Overall, the
413 dynamical evolution of the model is in good agreement with the observations. For
414 instance, January undergoes two major episodes of enhanced SO_2 that the model
415 reproduces well. Although there is a clear overestimation during some periods,
416 the model is able to reproduce the variations of the daily mean concentrations.

417 As regard to the scatter plot (Fig. 3f), 54.3% of the model results match with
418 observations within a factor of 2, and 90.1% within a factor of 5. The model re-
419 sults match the main tendency of the daily observations with an annual correlation

420 factor $r=0.60$.

421 The annual mean MNGE and MNBE values reach up to 118% and 83% re-
422 spectively (Table 3). Such rather high normalized errors are usual when evaluat-
423 ing background stations that measure very low values of SO_2 . The annual RMSE
424 is $2.2 \mu\text{g m}^{-3}$, much lower than for the other pollutants analyzed in the present
425 work. The seasonal statistics show better results for spring, with mean MNGE
426 value of 96%. The MNBE values increase for summer and fall as the daily mean
427 observations remain below $2 \mu\text{g m}^{-3}$.

428 The spatial distribution of the correlation coefficient r shows a large variabil-
429 ity per station. For instance, during winter while some northern stations have
430 high correlations ($0.6 < r < 0.9$), various low correlations are observed in central
431 and southern Europe. During summertime the correlation improves in stations lo-
432 cated over central Europe. In Spain, the model performs relatively homogeneously
433 across the year, with a variation of the correlation between summer and winter less
434 pronounced than in central Europe. However, the correlation per station in Spain
435 is slightly lower than in the rest of Europe, especially during summer.

436 Considering the mean bias for winter and summer (Fig. 5), results show a low
437 bias across all stations. Only one station located in eastern Poland displays a high
438 positive bias ($> 5 \mu\text{g m}^{-3}$ in summer). This station may largely contribute to the
439 seasonal and annual average positive bias mentioned in Table 3. The uncertainties
440 of the emission inventory in eastern Europe may be associated to the higher bias
441 observed in some stations of Poland and the Czech Republic, especially in winter.
442 Also, the top-down disaggregation from 50 to 12 km is a source of uncertainties
443 to be considered.

444 3.1.4. Particulate matter

445 A total of 16 and 25 stations are used to evaluate the simulated $\text{PM}_{2.5}$ and
446 PM_{10} concentrations, respectively. Although the model presents a clear sys-
447 tematic negative bias, it has noticeable capabilities to reproduce the dynamics
448 of $\text{PM}_{2.5}$ for the whole year (Fig. 3g). The modeling system simulates the most
449 important $\text{PM}_{2.5}$ episodes across the whole year. The correlation coefficients
450 for winter and fall seasons are 0.62 and 0.52, respectively, and 0.50 and 0.49 for
451 spring and summer (Table 3). The MFE and MFB for $\text{PM}_{2.5}$ do not fall within the
452 performance criteria or performance goal proposed by Boylan and Russell (2006).

453 In order to evaluate the annual variability of PM in comparison to measure-
454 ment data, Fig. 6 displays the annual time series of $\text{PM}_{2.5}$ and PM_{10} multiplied
455 by a correction factor of 2. Such correction is not meant to modify the statistics
456 but rather to evaluate the annual dynamics of the model and approximate the un-

Table 4: Seasonal and annual statistics obtained with CALIOPE-EU over Europe for 2004 (see Table 3). For quantification purposes, the simulated concentrations of PM are multiplied by a correction factor of 2 at the EMEP stations.

	Period	Data points	Measured mean	Modeled mean	r	MB	RMSE	MNBE	MNGE	MFB	MFE
PM2.5 daily adapted ($\times 2$) (16 stations)	Winter	1171	13.7	9.6	0.62	-3.3	12.4	6	60	-20	58
	Spring	1264	12.2	10.4	0.50	-1.3	10.0	1	49	-19	47
	Summer	1396	12.2	13.6	0.49	1.3	13.0	10	52	-10	45
	Fall	1287	11.5	12.3	0.52	1.5	11.4	22	58	-1	47
	Annual (no threshold)	5118	12.3	11.5	0.47	-0.3	11.8	10	54	-12	49
	Annual (threshold)	4756	13.0	12.6	0.45	-0.4	12.2	7	53	-14	49
PM10 daily adapted ($\times 2$) (25 stations)	Winter	1994	18.0	13.3	0.54	-4.3	14.7	6	61	-21	57
	Spring	2087	17.7	14.2	0.54	-3.4	12.4	-7	46	-25	48
	Summer	2204	18.5	16.3	0.60	-2.4	14.8	-7	46	-23	49
	Fall	2104	17.0	16.1	0.62	-0.9	12.1	13	56	-10	49
	Annual (no threshold)	8389	17.8	15.0	0.57	-2.7	13.6	1	52	-20	51
	Annual (threshold)	7918	18.7	15.6	0.55	-3.1	13.9	-5	48	-23	50

457 derestimation of PM mass. By multiplying the model results by such a factor, the
 458 results of the model system are in very good agreement with observations. The
 459 model is able to reproduce the daily evolution of PM2.5 across the year. Neverthe-
 460 less, the model tends to underestimate the peaks during wintertime, while during
 461 summertime the model overestimates some episodes. By calculating the annual
 462 MFE and MFB with the adapted model output, the results now fall within the
 463 performance goal recommended by Boylan and Russell (2006) with a MFE=49%
 464 and MFB=-12% (Table 4). It is important to note that the statistics are biased
 465 towards measurements obtained in Spain, since 10 out of 16 EMEP stations are
 466 located there (Fig. 4 and Fig. 5). Overall, the MFB and MFE are homogeneous at
 467 most stations (not shown).

468 For PM10, annual correlations are higher than for PM2.5 (annual mean cor-
 469 relation $r=0.57$). The model is able to reproduce most of the particulate matter
 470 events, although the model hardly reproduces the amplitude of the events and
 471 presents a systematic underestimation. Concerning the variability of the results
 472 (Fig. 3j), 69.4% of the data match with observations within a factor 2, and 96.6%
 473 within a factor 5. As for PM2.5, PM10 results present a very good agreement with
 474 the observations if a factor of 2 is applied to the results (Fig. 6b). The adapted re-
 475 sults for PM10 match consistently with the observations except for the Saharan
 476 dust outbreak event on July 24-26th which affected southern, central and eastern

477 Spain but was not captured by BSC-DREAM8b.

478 The annual mean MFB and MFE of the adapted results amount to -20% and
479 51%, respectively (Table 4). These results are in accordance with the recom-
480 mendations for particulate matter mentioned in Sect. 2.4 and fall within the per-
481 formance criteria of Boylan and Russell (2006). The spatial distribution of the
482 correlation coefficient and the mean bias for winter and summer point out that
483 the model performs better in southern than in northern Europe, for PM10 (Fig. 4
484 and Fig. 5). Stations located between the Baltic and the North Sea (DE01, DE09,
485 DK05; see Table 1) display weak seasonal correlation coefficient ($-0.1 < r < 0.3$).
486 However, continental stations of central Europe (Germany, Switzerland and Aus-
487 tria) mainly affected by anthropogenic emissions present good performances for
488 PM10. Correlations are in the range of 0.3-0.7 during winter and improves in
489 summer. From all coastal sites affected by SSA, the stations in Spain display the
490 highest correlations (Niembro and Cabo de Creus with $0.4 < r < 0.6$). At the
491 south European stations affected by Saharan dust outbreaks, namely Spain and
492 Italy, correlations are high across the year ($0.5 < r < 0.9$, except ES13). The
493 inclusion of BSC-DREAM8b model results largely contributes to the improve-
494 ment of the model performances at such southern stations as previously noted by
495 Jiménez-Guerrero et al. (2008).

496 Many studies have recognized the difficulty of models to simulate the mass
497 of particulate matter over Europe (van Loon et al., 2004; Matthias, 2008). The
498 underestimation of total particulate mass is, among others, the result from the lack
499 of fugitive dust emissions, resuspended matter (Vautard et al., 2005a), a possible
500 underestimation of primary carbonaceous particles (Schaap et al., 2004; Tsyro,
501 2005), the inaccuracy of SOA formation (Simpson et al., 2007), the difficulty of
502 representing primary PM emission from wood burning and other sources (Tsyro
503 et al., 2007) and a more general lack of process knowledge (Stern et al., 2008).
504 While multiplying the model results of CALIOPE-EU by a factor of 2, it was
505 shown that the dynamics of particulate matter (both PM2.5 and PM10) can be well
506 captured. Using such methodology the levels generally simulated by CALIOPE-
507 EU were quantified to be approximately half of the observed values.

508 3.2. Pattern Description

509 In the following section, it is important to note that the description of the
510 simulated chemical patterns does not take into account the model-observations
511 discrepancies highlighted in Sect. 3.1.

512 3.2.1. Ozone

513 Modeled O_3 average concentrations over Europe (Fig. 7a) show an increasing
514 gradient from the northern and western boundaries to the more continental and
515 Mediterranean areas, resulting from large variations in climate patterns (Beck and
516 Grennfeld, 1993; Lelieveld et al., 2002; EEA, 2005; Jiménez et al., 2006). In the
517 troposphere O_3 has a residence time of several days to a week which permits its
518 transport on regional scales (Seinfeld and Pandis, 1998). The highest concentra-
519 tions are found in the Mediterranean basin and southern Europe (nearly 90-105 μg
520 m^{-3}), as this region is particularly affected by intense photochemical production
521 of O_3 (EEA, 2005; Vautard et al., 2005b). Detailed descriptions of ozone for-
522 mation and transport over the Mediterranean area can be found in Gerasopoulos
523 et al. (2005) or Cristofanelli and Bonasoni (2009). Other important factor for the
524 land-sea difference is the slow dry deposition of O_3 on water and also the low pho-
525 tochemical formation due to the low precursors concentration (Wesely and Hicks,
526 2000). In central and eastern Europe, simulated annual O_3 concentrations range
527 from 70 to 85 $\mu\text{g m}^{-3}$, with a slight west-to-east gradual build-up caused by the
528 association of precursor emissions and predominant westerly winds. Northwest-
529 ern areas show rather low concentrations of O_3 (60-67 $\mu\text{g m}^{-3}$) due to reduced
530 solar radiation and the influence of the clean marine air. Due to higher O_3 con-
531 centrations in elevated terrains, the major mountainous regions such as the Alpine
532 and Pyrenean chains as well as the Carpathian mountains (mainly in Rumania)
533 display mean O_3 concentrations in the range of 85-95 $\mu\text{g m}^{-3}$. The minimum
534 values of O_3 (50-55 $\mu\text{g m}^{-3}$) are found in regions of chemically-driven high- NO_x
535 regime such as large polluted cities or within the shipping routes, Great Britain
536 and The Netherlands, and in northernmost Europe due to the association of low
537 precursor emissions and polar-like weather types. The O_3 distribution described
538 in this section is in accordance with the EMEP model results for the year 2005
539 presented by Tarrasón et al. (2007). However, the rather coarse resolution used
540 by the EMEP model (50 km \times 50 km) led to a less accurate simulation of the
541 chemical transition between urban and background areas.

542 3.2.2. Nitrogen dioxide

543 High concentrations of NO_2 within the PBL are directly related to anthro-
544 pogenic emissions (EEA, 2007). The largest contributors to NO_2 atmospheric
545 concentrations are the emissions from road transport (40% of NO_2 total emission)
546 followed by power plants and other fuel converters (22% of NO_2 total emission,
547 Tarrasón et al., 2006). High modeled NO_2 concentrations (\sim 20-30 $\mu\text{g m}^{-3}$)
548 are reported in The Netherlands and Belgium, the industrial Po Valley (northern

Italy), central and eastern England, and the Ruhr region (western Germany). Various important European cities even reach NO_2 levels up to $30\text{-}40 \mu\text{g m}^{-3}$ on annual average (e.g., Milan, London, Paris). Suburban areas surrounding the major cities often undergo advections of polluted air masses and display mean annual values near $10\text{-}25 \mu\text{g m}^{-3}$ while clean regions unaffected by emissions rather have concentrations below $5 \mu\text{g m}^{-3}$. Also note that the major shipping routes originating from the North Sea, passing by the English Channel, through Portugal, Spain and northern Africa toward the Suez Canal substantially affect the coastal NO_2 concentrations with a maximum of $18 \mu\text{g m}^{-3}$ for the annual mean concentrations. Qualitative comparisons between the simulated pattern of annual NO_2 and satellite-derived NO_2 tropospheric column densities from GOME (Beirle et al., 2004), SCIAMACHY and OMI (Boersma et al., 2007) revealed good agreement (not shown). Such finding demonstrates the relative accuracy in the spatial description of the source regions and various European hot-spots.

3.2.3. Sulfur dioxide

Simulated SO_2 annual average concentrations over Europe (Fig. 7c) show highest levels over northwestern Spain, eastern Europe (Poland, Serbia, Rumania, Bulgaria and Greece), and over UK, Belgium and the southwestern part of The Netherlands. Combustion emissions from power plants and transformation industries are the main responsible for such high concentrations of SO_2 over Europe. 64% of SO_2 total emissions are attributed to these sectors (Tarrasón et al., 2006). The highest annual concentrations ($\sim 70\text{-}90 \mu\text{g m}^{-3}$) are observed in northern Spain due to the presence of two large power plant installations. However, background regions in Spain remain below mean concentrations of $2 \mu\text{g m}^{-3}$. On the other hand, east European countries are affected by higher background concentrations of SO_2 (~ 8 to $20 \mu\text{g m}^{-3}$) with various punctual emissions contributing to an increase of the regional concentrations (~ 30 to $50 \mu\text{g m}^{-3}$). Over sea, the highest concentrations are found along the main shipping routes, as emissions from ships largely contribute to the SO_x concentrations due to combustion of fuels with high sulfur content (Corbett and Fischbeck, 1997; Corbett and Koehler, 2003).

The distribution of mean annual SO_2 concentrations for 2004 shows the same pattern as that presented by Tarrasón et al. (2007) for 2005. However, note that the SO_2 levels have decreased according to the pattern shown in Schaap et al. (2004) for the year 1995. Indeed, from the mid-1990s to 2004, SO_2 concentrations in air have strongly decreased due to reductions in SO_x emissions. SO_x emissions have reduced up to 50% mainly in the sectors of power and heat generation through a combination of using fuels with lower sulfur content (such as switching from

586 coal and oil to natural gas) and implementing emission abatement strategies in the
587 energy supply and industry sectors (EEA, 2007; International Maritime Organiza-
588 tion and Marine Environment Protection Committee, 2001).

589 3.2.4. Particulate matter

590 The simulated spatial distribution of annual mean PM_{2.5} (Fig. 7d) shows av-
591 erage background levels around 3-10 $\mu\text{g m}^{-3}$ in northwestern, central and eastern
592 Europe. Very low concentrations correspond to remote marine air and the ma-
593 jor European mountain chains (e.g., the Alps, Massif Central, the Pyrenees and
594 the Carpathians). The concentration levels are dominated by SIA, namely sulfate,
595 nitrate and ammonium (not shown here). SSA does not substantially contribute
596 to the PM_{2.5} fraction. The most polluted European region is the Po Valley with
597 annual mean values near 14-22 $\mu\text{g m}^{-3}$. To a lesser extent, in the Benelux re-
598 gion (Belgium, The Netherlands, Luxembourg) high concentrations of PM_{2.5} are
599 found (\sim 8-12 $\mu\text{g m}^{-3}$). Such concentrations are mainly associated with primary
600 anthropogenic emissions from road traffic and secondary aerosols. As mentioned
601 in Sect. 3.2.3 Bulgaria, Rumania and Poland are important contributors of SO₂.
602 At the hot-spot locations, the large sulfate formation and primary PM emissions
603 lead to annual mean concentrations of up to 20-22 $\mu\text{g m}^{-3}$. Interestingly, the large
604 sources of SO₂ located in eastern UK and northwestern Spain do not contribute
605 efficiently to the PM_{2.5} formation. Such low sulfate formation is most likely
606 caused by high dispersion and strong removal by wet deposition in these regions.
607 The north African continent constitutes a very large potential source of PM for
608 the rest of the domain. During episodes of Saharan dust outbreaks, mineral dust
609 largely contributes to the levels of PM_{2.5} in southern Europe.

610 Fig. 8a and Fig. 8b present the annual mean and 1-hour maximum of PM₁₀
611 concentrations in Europe, respectively. PM₁₀ includes the PM_{2.5} fraction, the
612 primary anthropogenic coarse fraction (PM_{10-2.5}), as well as the contribution of
613 coarse SSA and Saharan dust. Among other uncertainties, wind-blown or re-
614 suspended dust emissions (coarse fraction) are not taken into account yet. Such
615 sources contribute to the underestimation of the total concentrations of PM₁₀,
616 especially in dry regions or in urban areas (see Amato et al., 2009a,b).

617 High mean and maximum values of annual PM₁₀ concentrations found in the
618 North Sea and the nearshore Atlantic result from SSA production. The mean con-
619 tribution of SSA in the Mediterranean Sea reaches around 10 $\mu\text{g m}^{-3}$. The annual
620 mean contribution of the anthropogenic coarse fraction remains low (\sim 5 $\mu\text{g m}^{-3}$)
621 and is located at or in the vicinity of important emission sources (not shown). Sa-
622 haran dust is responsible for the very high levels of PM in northern Africa and

623 also regularly affects the Mediterranean basin and southern Europe. Spain, south-
624 ern France, Italy, and Greece are particularly affected by such episodes. Fig. 8b
625 reflects well the importance of including Saharan dust model data (on a non-
626 climatic basis) since dust outbreaks lead to annual maximum concentrations of
627 PM10 greater than $300 \mu\text{g m}^{-3}$ in most of the territories surrounding the Mediter-
628 ranean Sea.

629 Qualitatively, the spatial distributions of PM2.5 and PM10 show similar pat-
630 terns to distributions found in other European modeling studies including sea salt
631 and Saharan dust emissions (see, e.g., POLYPHEMUS and the Unified EMEP
632 model, Sartelet et al., 2007; Tarrasón et al., 2006). Substantial differences arise
633 in concentrations over southern Europe when comparing spatial distributions with
634 models not taking dust from the African continent into account (see Bessagnet
635 et al., 2004).

636 4. Comparison with Other Evaluation Studies

637 There are several air pollution modeling systems on the European scale op-
638 erated routinely in Europe. Evaluations of these regional air quality models with
639 ground-based measurements were carried out either individually or in compari-
640 son to other models. The following discussion presents a comparative analysis
641 between various European model evaluations and CALIOPE-EU. This analysis
642 does not attempt to be an intercomparison study because the studies were per-
643 formed under different conditions (simulated year, meteorological data, boundary
644 conditions, emissions, etc.). However, it provides a good basis for assessing the
645 reliability of the results obtained in the context of the European evaluation mod-
646 els. Table 5 shows a chronological list of published evaluation studies, which are
647 presented along with CALIOPE-EU evaluation results.

648 The presented evaluation studies have several characteristics in common. First,
649 they were carried out over Europe on a regional scale with horizontal resolutions
650 in the range of $25\text{-}55 \text{ km} \times \text{km}$. Second, the simulations were run over a long
651 period, mainly a year. The given models were evaluated against ground-based ob-
652 servations at rural locations from EMEP or AIRBASE databases. Also note that
653 these evaluation studies were performed using statistical methods.

654 Most of the studies presented here, evaluated independently in previous pub-
655 lications, focused on both gas and particulate phases. These studies comprise:
656 LOTOS-EUROS (Schaap et al., 2008), POLYPHEMUS (Sartelet et al., 2007),
657 Unified EMEP (Tarrasón et al., 2006; Yttri et al., 2006), and CHIMERE (Bessag-
658 net et al., 2004; Schmidt et al., 2001). In the case of the Unified EMEP model,

Table 5: List of published European model evaluation studies and their main characteristics to be compared with CALIOPE-EU evaluation results (this study). A study code for each model is specified to ease the discussion in this paper.

Reference	Modeled year	Model name	Horizontal resolution /layers	Study code
This study	2004	CALIOPE-EU	12 km × 12 km/15	CALIOPE-EU04
Matthias (2008)	2001	CMAQ	54 km × 54 km/20	CMAQ2
Schaap et al. (2008)	1999	LOTOS-EUROS	25 km × 25 km	LOTOS-EUROS3
Sartelet et al. (2007)	2001	POLYPHEMUS	0.5° × 0.5°/5	POLYPHEMUS4
van Loon et al. (2007)	1999	Unified EMEP	50 km × 50 km/20	EMEP5
van Loon et al. (2007)	1999	RCG	0.5° × 0.5°/5	RCG5
van Loon et al. (2007)	1999	LOTOS-EUROS	0.5° × 0.5°/4	LOTOS-EUROS5
van Loon et al. (2007)	1999	CHIMERE	0.5° × 0.5°/8	CHIMERE5
van Loon et al. (2007)	1999	MATCH	0.4° × 0.4°/14	MATCH5
Tarrasón et al. (2006)	2004	Unified EMEP	50 km × 50 km/20	EMEP6
Yttri et al. (2005)	2004	Unified EMEP	50 km × 50 km/20	EMEP7
Bessagnet et al. (2004)	1999	CHIMERE	0.5° × 0.5°/8	CHIMERE8
van Loon et al. (2004)	1999/2001	CHIMERE	0.5° × 0.5°/8	CHIMERE9
van Loon et al. (2004)	1999/2001	DEHM	50 km × 50 km/20	DEHM9
van Loon et al. (2004)	1999/2001	Unified EMEP	50 km × 50 km/20	EMEP9
van Loon et al. (2004)	1999/2001	MATCH	55 km × 55 km/10	MATCH9
van Loon et al. (2004)	1999/2001	LOTOS	0.25° × 0.5°/3	LOTOS9
van Loon et al. (2004)	1999/2001	CMAQ	36 km × 36 km/21	CMAQ9
van Loon et al. (2004)	1999/2001	REM-CALGRID	0.25° × 0.5°	REM-CALGRID9
Schaap et al. (2004)	1995	LOTOS	25 km × 25 km/3	LOTOS10
Hass et al. (2003)	1995	DEHM	50 km × 50 km/10	DEHM11
Hass et al. (2003)	1995	EURAD	27 km × 27 km/15	EURAD11
Hass et al. (2003)	1995	EUROS	0.55° × 0.55°/4	EUROS11
Hass et al. (2003)	1995	LOTOS	0.25° × 0.5°/3	LOTOS11
Hass et al. (2003)	1995	MATCH	55 km × 55 km/10	MATCH11
Hass et al. (2003)	1995	REM3	0.25° × 0.5°	REM11
Schmidt et al. (2001)	1998	CHIMERE	0.5° × 0.5°/5	CHIMERE12

659 evaluation studies are being processed every year since 1980 (Tarrasón et al.,
660 2005). For the purpose of this paper, we only exploited their evaluation of the
661 year 2004, since it is the reference year modeled by CALIOPE-EU. The single
662 evaluations of both CMAQ (Matthias, 2008) and LOTOS (Schaap et al., 2004)
663 only focused on particulate matter results.

664 In addition to the models evaluated independently and listed above, three
665 model intercomparisons were also carried out and are presented in Table 5. In
666 the framework of EUROTRAC (Hass et al., 2003) the authors evaluated the abil-
667 ity of six models to simulate inorganic aerosol compounds. In the review of the
668 Unified EMEP model (van Loon et al., 2004) the gas and particulate phases from
669 seven models were compared. More recently, an intercomparison was performed
670 in order to study the response of five models to different emission scenarios in
671 terms of O₃ levels (EURODELTA project, van Loon et al., 2007).

672 Table 6 and Table 7 present the statistics of each reviewed study available for
673 the gas (O₃, NO₂ and SO₂) and particulate (PM10 and PM2.5) phases, respec-
674 tively. Three statistical parameters are considered, namely the annual daily means
675 of MNBE, r, and RMSE. These parameters were calculated without threshold on
676 the measurement data, except for the MNBE value of O₃ in POLYPHEMUS4
677 which is calculated using a threshold of 80 μg m⁻³ as pointed out by Sartelet
678 et al. (2007). The displayed results represent the annual means at all considered
679 stations. Values in parentheses, when available, correspond to the minimum and
680 maximum performances at individual stations.

681 For the O₃ daily mean CALIOPE-EU presents satisfactory annual MNBE val-
682 ues in comparison to the other studies (6 μg m⁻³ versus 2-29 μg m⁻³). The
683 annual daily mean correlation is rather low (0.66 versus 0.53-0.83). Nevertheless,
684 the RMSE obtained with CALIOPE-EU is in the range of other models (20.6 μg
685 m⁻³ for CALIOPE-EU versus 18.4-28.1 μg m⁻³). Values for the annual daily
686 peak mean correlations for CALIOPE-EU are slightly below the range of the
687 other studies. Note that the CMAQ9 model obtained the same annual daily peak
688 mean correlation as CALIOPE-EU, namely 0.69 versus 0.71-0.84, which is lower
689 than in the other studies. However, for individual stations, CALIOPE-EU remains
690 within the same range of EMEP6 for the year 2004 (0.28-0.82 versus 0.10-0.84).
691 This large range of values reflects the high variability of the model performances
692 depending on the region of the domain (see Fig. 4 and discussion in Sect. 3.1.1).
693 RMSE and MNBE values for annual daily peak mean of O₃ lie within the range
694 of the other models.

695 Overall, the CALIOPE-EU performances for NO₂ are superior to other mod-
696 els. The annual daily mean correlation obtained in this study is the highest from

Table 6: Comparison of the statistics Mean Normalized Bias Error (MNBE, %), correlation (r), and Root Mean Squared Error (RMSE, $\mu\text{g m}^{-3}$) between CALIOPE-EU and other European models^{a,b} for gas phase (O₃, NO₂ and SO₂ daily and O₃ daily peak). The statistics do not consider thresholds on measurement data except for the MNBE value (*) provided by the POLYPHEMUS study.

Study Number	O ₃ daily average			O ₃ daily peak average			NO ₂ daily average			SO ₂ daily average		
	MNBE	r	RMSE	MNBE	r	RMSE	MNBE	r	RMSE	MNBE	r	RMSE
CALIOPE-EU04	6	0.66	20.6	-3	0.69	21.8	-17	0.67	10.1	83	0.60	2.2
	(-22, 43)	(0.06, 0.81)	(15.8, 29.2)	(-23, 23)	(0.28, 0.82)	(17.5, 30.7)	(-74, 77)	(0.02, 0.84)	(1.4, 36.3)	(-28, 370)	(0.13, 0.80)	(0.8, 6.4)
LOTOS-EUROS3		0.65	25.2		0.75	20.4		0.40	11.4		0.40	3.4
POLYPHEMUS4				-14*	0.72	21.4		0.33	10.0		0.47	5.0
EMEP5	10	0.72		1	0.75							
RCG5	3	0.71		7	0.76							
LOTOS-EUROS5	2	0.7		7	0.76							
CHIMERE5	29	0.76		10	0.84							
MATCH5	6	0.8		2	0.81							
EMEP6	10	0.72		1	0.75					0.67		
					(0.10, 0.84)							
CHIMERE8							(-78, 349)	(-0.30, 0.70)	(1.0, 28.0)			
CHIMERE9		0.78/0.83	18.4/18.1		0.78/0.83	18.4/18.1		0.47/0.44	12.6/13.9		0.37/0.47	10.9/10.1
DEHM9		0.66/0.66	24.2/23.1		0.78/0.78	22.1/21.7		0.45/0.46	11.1/11.7		0.43/0.49	4.8/3.9
EMEP9		0.63/0.65	23.6/23.0		0.75/0.76	19.1/19.5		0.43/0.45	11.2/12.1		0.40/0.42	4.7/3.9
MATCH9		0.65/0.68	24.7/24.5		0.79/0.80	18.3/18.8		0.42/0.44	11.8/12.5		0.43/0.48	4.4/3.2
LOTOS9		0.53/0.54	27.7/28.1		0.74/0.73	21.7/22.0		0.25/0.30	12.9/13.6		0.24/0.45	5.9/4.6
CMAQ9		0.55/-	32.6/-		0.69/-	25.5/-		0.52/-	10.8/-		0.44/-	6.0/-
REM-CALGRID9		0.61/0.64	26.4/25.7		0.71/0.74	21.9/22.0		0.40/0.42	11.9/12.6		0.35/0.39	4.7/3.5
LOTOS10											0.48	4.1
DEHM11								0.23	8.7		0.43	2.8
EURAD11								0.16	8.9		0.39	5.6
EUROS11								0.07	9.4		0.39	3.9
LOTOS11								0.03	9.2		0.39	3.1
MATCH11								0.23	8.5		0.45	2.7
REM311								0.13	9.3		0.35	3.3
CHIMERE12					(0.51, 0.88)	(13.4, 44.6)		(-0.05, 0.77)	(1.0, 10.0)			

^a Value reported without parenthesis represents the annual average in the entire domain. The first and second values in parenthesis represent the minimum and maximum values respectively obtained among all stations in the entire domain. ^b Values reported before and after a slash correspond to the year 1999 and 2001, respectively.

Table 7: Comparison of the statistics MNBE (%), r and RMSE ($\mu\text{g m}^{-3}$) between CALIOPE-EU and other European models^{a,b} for particulate matter PM2.5 and PM10. The statistics do not consider thresholds on measurement data.

Study Number	PM2.5 daily average			PM10 daily average		
	MNBE	r	RMSE	MNBE	r	RMSE
CALIOPE-EU04	-45 (-68, -13)	0.47 (0.46, 0.79)	11.2 (5.5, 25.3)	-50 (-72, 12)	0.57 (0.10, 0.77)	15.8 (5.7, 31.4)
CMAQ2					(0.35, 0.69)	
POLYPHEMUS4		0.54	8.6		0.54	12.6
EMEP7		0.44 (0.28, 0.7)	10.6		0.48 (0.24, 0.66)	14.1
CHIMERE8				(-80, 20)	(0.50, 0.70)	(0.8, 30.0)
CHIMERE9					0.55/0.55	14.4/13.8
DEHM9					0.50/0.49	16.0/14.5
EMEP9					0.52/0.48	15.7/14.9
MATCH9					0.44/0.49	14.9/12.9
LOTOS9					0.45/0.38	16.6/15.2
CMAQ9					0.54/-	15.0/-
REM-CALGRID9					0.57/0.49	13.2/12.4
LOTOS10					(0.35, 0.69)	

^a Value reported without parentheses represents the annual average in the entire domain. The first and second values in parenthesis represent the minimum and maximum values respectively obtained among all stations in the entire domain. ^b Values reported before and after a slash correspond to the year 1999 and 2001, respectively.

697 all considered models (0.67 versus 0.03-0.47). The annual daily mean RMSE
698 value is among the lowest ($10.0 \mu\text{g m}^{-3}$ versus $8.5\text{-}13.9 \mu\text{g m}^{-3}$). MNBE val-
699 ues for CALIOPE-EU are similar to CHIMERE8, the only study providing NO_2
700 annual daily mean values. Such a broad range of MNBE values is caused by
701 the sensitivity to low observed concentrations, inducing problems of inflation and
702 asymmetry (Yu et al., 2006). Therefore, we encourage future modeling studies to
703 use threshold-filtered MNBE for NO_2 or else use fractional errors instead. The
704 high performances of CALIOPE-EU with NO_2 is attributed mostly to the high
705 resolution of the model system which enables a well-defined spatial and temporal
706 description of NO_2 sources throughout Europe.

707 As with NO_2 , the CALIOPE-EU evaluation results for SO_2 show very satis-
708 factory performances in comparison to the other studies. The calculated RMSE
709 is the lowest from all models ($2.2 \mu\text{g m}^{-3}$ against $2.7\text{-}10.9 \mu\text{g m}^{-3}$). Addition-
710 ally the annual daily mean correlation obtained for CALIOPE-EU is the second
711 highest value after the EMEP6 study with $r=0.60$ against 0.67, respectively. The
712 other studies calculated lower correlation coefficients between 0.24 and 0.49. No
713 annual daily mean MNBE values were provided by the other evaluations. Also,
714 the SO_2 model performances are mainly attributed to the high resolution of the
715 CALIOPE-EU system enhancing the simulation accuracy. As mean background
716 concentrations of observed SO_2 in Europe are low ($\sim 2 \mu\text{g m}^{-3}$, see Table 3), mean
717 normalized errors may not adequately represent the performances of a model at
718 rural sites. In that case, the use of thresholds on observational data or rather MFE
719 and MFB should be considered.

720 Considering $\text{PM}_{2.5}$, the model performance on the annual mean correlation
721 coefficient is comparable with the two other studies POLYPHEMUS4 and EMEP7
722 (0.49 versus 0.44 and 0.54). Such correlation is rather low and reflects the high
723 uncertainties in the sources of fine particles (see discussion in Sect. 3.1.4). The
724 annual daily mean RMSE obtained by CALIOPE-EU is slightly higher than the
725 values obtained by the two other studies ($11.0 \mu\text{g m}^{-3}$ versus 8.6 and $10.6 \mu\text{g}$
726 m^{-3}).

727 Statistics for PM_{10} are in the same range as for the other studies. As with
728 all other models, CALIOPE-EU tends to underestimate the PM_{10} concentrations,
729 with the calculation of $\text{PM}_{2.5}$ concentrations being a substantial source of un-
730 derestimation. Per individual stations, the MNBE range for CALIOPE-EU is
731 similar to that of CHIMERE8 (from -72% to 12% compared to -80% to 20%
732 for CHIMERE8). The calculated annual daily mean correlation coefficient of
733 this work is the highest value from all other studies, together with the REM-
734 CALGRID9 study for the year 1999. The annual daily mean RMSE remains in

735 the range of other studies ($15.7 \mu\text{g m}^{-3}$ versus $12.4\text{-}16.6 \mu\text{g m}^{-3}$)

736 Overall, the performances on the levels and variability of particulate matter are
737 relatively poor, but this intercomparison shows that the underestimated mean con-
738 centrations and the lack of understanding on the formation processes is a general
739 feature affecting most models.

740 The results of this intercomparison suggest that CALIOPE-EU performs rel-
741 atively well for the simulation of O_3 concentrations while high scores were ob-
742 tained for NO_2 and SO_2 . In general, performances on particulate matter (PM_{2.5}
743 and PM₁₀) are satisfactory in comparison to the other studies. However, substan-
744 tial efforts should be made in the chemical description of PM formation and the
745 accuracy of PM sources.

746 From this model inter-comparison it was noticed that model systems based
747 on the CMAQ chemical model (CALIOPE-EU and CMAQ9) perform better for
748 daily mean NO_2 and SO_2 than for O_3 daily average and daily peak averages when
749 compared to the other systems. While most European models obtain O_3 annual
750 mean daily peak correlations between 0.7 and 0.8 for the year 2004, both CMAQ
751 models reach a maximum of 0.69. However, note that this correlation obtained
752 by CALIOPE-EU is higher than values reported by other studies using CMAQ
753 and representing the US domain (see, e.g., Zhang et al., 2006; Yu et al., 2006;
754 Eder and Yu, 2006). On the other hand, the correlations for NO_2 and SO_2 are
755 notably higher for CMAQ models than for the other chemical models. All models
756 are based on the same emissions from the EMEP database, but the disaggregation
757 techniques or additional integrated modules may differ. These results indicate
758 some potential limitations with the chemical mechanism used within this version
759 of CMAQ (CBM-IV) when applied to the EMEP emissions over Europe (also
760 see Emmerson and Evans, 2009). The Carbond Bond mechanism has recently
761 been updated (Yarwood et al., 2005) and evaluated (Luecken et al., 2008). It is
762 expected that the latest mechanism, namely CB05, could improve the behaviour
763 of the CMAQ model over rural European areas considering the efforts done to
764 improve the simulations under low NO_x conditions.

765 Another relevant issue that arises from the model comparison is the impact
766 of horizontal resolution. As stated before in the text, all models are forced with
767 EMEP emissions. These emissions have a spatial resolution of $50 \text{ km} \times 50 \text{ km}$.
768 After different spatial disaggregation techniques most models perform similarly
769 regardless of the target horizontal resolution. This result is not surprising if one
770 considers that this evaluation focuses on rural environments limited by NO_x . The
771 horizontal resolution may impact urban and industrial areas at a higher degree
772 than rural areas. In this sense, the higher horizontal resolution of CALIOPE-

773 EU system may be responsible for the better scores obtained in NO₂ and SO₂.
774 It is reasonable to think that a detailed emission inventory at a finer horizontal
775 resolution could further improve the air quality model performances.

776 Finally, the vertical resolution of the models presented in this evaluation ranges
777 from 3 to 20 vertical layers. It is expected that models with higher vertical lev-
778 els are able to simulate the vertical mixing better. However, the statistics do not
779 show a direct relationship with the model vertical resolution. That implies that
780 various systems are strongly driven by surface emissions, and vertical exchange
781 is not directly resolved though strongly parameterized.

782 5. Conclusions

783 This paper presented the evaluation results of the model system CALIOPE-
784 EU (namely WRF-ARW/HERMES-EMEP/CMAQ/BSC-DREAM8b) using a full
785 year simulation for 2004 over a European domain. The evaluation focused on
786 the capability of the model to reproduce the temporal and spatial distribution of
787 pollutants, estimating their uncertainty and comparing them with other European
788 evaluation studies. This article evaluated gas (O₃, NO₂ and SO₂) and particulate
789 phase (PM₁₀ and PM_{2.5}) simulations with EMEP ground-based measurements. It
790 is noteworthy mentioning that neither correction factors nor any adjusting model
791 parameterization were applied to the model output or the original model codes.
792 Only in the case of particulate matter, adjusted levels were discussed in order to
793 quantify the missing source apportionment.

794 CALIOPE-EU was able to reproduce the observed O₃ annual cycle. More-
795 over, CALIOPE-EU simulated the general features of O₃ fields over Europe, es-
796 pecially the differences between urban and background levels. In general, daily
797 maxima were better simulated than daily averages, and summertime concentra-
798 tions were better simulated than wintertime concentrations. The conditions at the
799 lateral boundaries of the model domain were shown to strongly affect the evo-
800 lution of O₃ throughout the year, especially at the stations near the boundaries
801 and during wintertime. These conditions should be handled with care, as they
802 occasionally lead to excessive O₃ concentrations near the surface. In CMAQ, the
803 construction of boundary profiles from global chemistry models, in that case the
804 LMDz-INCA2, should integrate the information of the tropopause in the down-
805 scaling process to avoid strong downdrafts of O₃-enriched air masses down to the
806 surface.

807 Concerning NO₂, the annual trend was moderately well simulated with a sys-
808 tematic negative bias. High correlations were obtained over either very clean or

809 highly polluted areas (stations around the Baltic Sea or UK). On average, the
810 model underestimated both background levels and peaks, especially during win-
811 ter and over high polluted areas where transport dominates compared to chemical
812 processes. From the results of the annual pattern, CALIOPE-EU was able to sim-
813 ulate maximum concentrations over most important emission sources in Europe,
814 since concentrations sharply decrease from urban-suburban to rural areas.

815 The model system was able to reproduce the annual variability of daily mean
816 concentrations for background SO_2 throughout Europe. Monthly variations of
817 SO_2 were well captured, especially from January to March, but false peaks were
818 reported. Vertical mixing characteristics and the way emissions are distributed
819 within the grid are potential key issues which may explain the overestimation
820 detected in simulated SO_2 . The spatial distribution of statistics showed low mean
821 bias values with heterogeneous correlation coefficients. The spatial SO_2 pattern
822 successfully represented the main European sources (in the vicinity of energy and
823 transformation industries and shipping routes).

824 By comparing model results with measurements of $\text{PM}_{2.5}$ and PM_{10} it was
825 found that CALIOPE-EU reproduces most of the pollution events. However, the
826 model underestimated the observed values of $\text{PM}_{2.5}$ and PM_{10} . In order to iden-
827 tify the origin of such discrepancies and to determine the sources of uncertainty,
828 the aerosol chemical composition should be evaluated. Among other sources not
829 accounted for, particulate matter emissions from paved road re-suspension and
830 wind blown dust should be included in order to reduce the systematic biases.
831 When a multiplying factor of 2 was applied to both simulated $\text{PM}_{2.5}$ and PM_{10} ,
832 MFE and MFB statistics lied within the performance goal defined by Boylan and
833 Russell (2006). Moreover, the contribution of seasonal natural particulate mat-
834 ter, marine and Saharan mineral dust, was well characterized. Introducing dust
835 aerosol outbreaks on a non-climatic basis with BSC-DREAM8b was essential for
836 the simulation of hourly peaks during dust outbreaks, especially in southern Eu-
837 rope.

838 When compared to other European models CALIOPE-EU performed reason-
839 ably well for ozone annual daily mean and daily peak concentrations. O_3 statis-
840 tics lie within the US-EPA guidelines although annual correlations are rather low
841 compared to other European models. On the other hand, statistics for NO_2 , SO_2 ,
842 PM_{10} and $\text{PM}_{2.5}$ present higher scores than most models. We noted a similar
843 behaviour with the other CMAQ-based modelling system; both systems present
844 lower annual correlations for O_3 while results of NO_2 , SO_2 , $\text{PM}_{2.5}$ and PM_{10} are
845 higher than other systems.

846 The horizontal resolution of CALIOPE-EU provided high details in the spa-

847 tial distribution and temporal evolution of most relevant gas-phase and particulate
848 matter pollutants. Sharp and concentrated plumes and other sub-grid scale pro-
849 cesses were represented correctly. Although emission data are based on the dis-
850 aggregation from the EMEP inventory (emissions at 50 km × 50 km), the results
851 are within the range of most European models.

852 This study warrants the use of the CALIOPE-EU system over Europe and
853 results will be used as boundary conditions for the high-resolution air quality sim-
854 ulation over the Iberian peninsula at a 4 km × 4 km resolution.

855 6. Acknowledgements

856 The authors wish to thank EMEP for the provision of measurement stations
857 and CIEMAT, CSIC-IJA, CEAM centers for their collaboration in the project.
858 Also, thanks to C. Pérez, E. Lopez and L. González for their work related to
859 the CALIOPE system as well as S. Szopa and A. Cozic for the provision of
860 LMDz-INCA2 chemical data. This work is funded by the CALIOPE project of
861 the Spanish Ministry of the Environment (441/2006/3-12.1, A357/2007/2-12.1,
862 157/PC08/3-12.0). All simulations were performed on the MareNostrum super-
863 computer hosted by the Barcelona Supercomputing Center.

864 References

- 865 Adams, L.I., Davis, J., Japar, S.M., Finley, D.R., 1990. Real-time, in situ mea-
866 surements of atmospheric optical absorption in the visible via photoacoustic
867 spectroscopy iv. visibility degradation and aerosol optical properties in los an-
868 geles. *Atmos. Environ.* 24A, 605610.
- 869 Amato, F., Pandolfi, M., Escrig, A., Querol, X., Alastuey, A., Pey, J., Perez, N.,
870 Hopke, P.K., 2009a. Quantifying road dust resuspension in urban environment
871 by multilinear engine: A comparison with pmf2. *Atmos. Environ.* 43, 2770–
872 2780.
- 873 Amato, F., Pandolfi, M., Escrig, A., Querol, X., Alastuey, A., Pey, J., Perez, N.,
874 Hopke, P.K., 2009b. Quantifying road dust resuspension in urban environment
875 by multilinear engine: A comparison with pmf2. *Atmos. Environ.* 43, 2770–
876 2780, doi:10.1016/j.atmosenv.2009.02.039.
- 877 Baldasano, J.M., Güereca, L.P., López, E., Gassó, S., Jimenez-Guerrero, P.,
878 2008a. Development of a high-resolution (1 km x 1 km, 1h) emission model

- 879 for spain: The high-elective resolution modelling emission system (hermes).
880 Atmos. Environ. 42, 7215–7233.
- 881 Baldasano, J.M., Jiménez-Guerrero, P., Jorba, O., Pérez, C., López, E., Güereca,
882 P., Martín, F., Vivanco, M.G., Palomino, I., Querol, X., Pandolfi, M., Sanz,
883 M.J., Diéguez, J.J., 2008b. Caliope: an operational air quality forecasting sys-
884 tem for the iberian peninsula, balearic islands and canary islands - first annual
885 evaluation and ongoing developments. Adv. Sci. Res. 2, 89–98.
- 886 Beck, J., Grennfeld, P., 1993. Distribution of ozone over europe, in: the Proceed-
887 ings of the EUROTRAC Symposium, pp. 43–58.
- 888 Beirle, S., Platt, U., Wenig, M., Wagner, T., 2004. Highly resolved global distribu-
889 tion of tropospheric NO₂ using gome narrow swath mode data. Atmos. Chem.
890 Phys. 4, 1913–1924.
- 891 Bessagnet, B., Hodzic, A., Vautard, R., Beekmann, M., Cheinet, S., Honoré, C.,
892 Liousse, C., Rouil, L., 2004. Aerosol modeling with chimere-preliminary eval-
893 uation at the continental scale. Atmos. Environ. 38, 2803–2817.
- 894 Binkowski, F.S., Roselle, S.J., 2003. Models-3 community multiscale air quality
895 (cmaq) model aerosol component. 1. model description. J. Geophys. Res. 108
896 (D6), 4183, doi:10.1029/2001JD001409.
- 897 Binkowski, F.S., 1999. Aerosols in models-3 cmaq, in: Byun, D.W., Ching, J.K.S.
898 (Eds.), Science Algorithms of the EPA Models-3 Community Multiscale Air
899 Quality (CMAQ) Modeling System, EPA. pp. 10–0 – 10–23.
- 900 Boersma, K.F., Eskes, H.J., Veefkind, J.P., Brinksma, E.J., van der A, R.J., Sneep,
901 M., van der Oord, G.H.J., Levelt, P.F., Stammes, P., Gleason, J.F., Bucsela, E.J.,
902 2007. Near-real time retrieval of tropospheric NO₂ from omi. Atmos. Chem.
903 Phys. 7, 2103–2118.
- 904 Boylan, J., Russell, A., 2006. Pm and light extinction model performance metrics,
905 goals, and criteria for three-dimensional air quality models. Atmos. Environ.
906 40, 4946–4959.
- 907 Byun, D.W., Ching, J.K.S., 1999. Science algorithms of the epa models-3 com-
908 munity multiscale air quality (cmaq) modeling system. Atmospheric modeling
909 division, National Exposure Research Laboratory, US Environmental Protec-
910 tion Agency, Research Triangle Park, NC 27711.

- 911 Byun, D., Schere, K.L., 2006. Review of the governing equations, computational
912 algorithms, and other components of the models-3 community multiscale air
913 quality (cmaq) modeling system. *Appl. Mech. Rev.* 59 (2), 51–77.
- 914 Chang, J.C., Hanna, S.R., 2004. Air quality model performance evaluation. *Me-
915 teorol. Atmos. Phys.* 87, 167–196.
- 916 Ching, J., Herwehe, J., Swall, J., 2006. On joint deterministic grid modeling
917 and sub-grid variability conceptual framework for model evaluation. *Atmos.
918 Environ.* 40, 4935–4945.
- 919 Chylek, P., Wong, J., 1995. Effect of absorbing aerosols on global radiation bud-
920 get. *Geophys. Res. Lett.* 22 (8), 929–931, doi:10.1029/95GL00800.
- 921 Corbett, J.J., Fischbeck, P., 1997. Emissions from ships. *Science* 278 (5339),
922 823–824, doi:10.1126/science.278.5339.823.
- 923 Corbett, J.J., Koehler, H.W., 2003. Updated emissions from ocean shipping. *J.
924 Geophys. Res.* 108 (D20), 4650, doi:10.1029/2003JD003751.
- 925 COST, 2009. Towards a European Network on Chemical Weather Forecasting
926 and Information Systems (ENCWF). Technical Report. COST Action ES0602,
927 Monitoring Progress Report.
- 928 Cox, W.M., Tikvart, J.A., 1990. Statistical procedure for determining the best
929 performing air quality simulation model. *Atmos. Environ.* 24, 2387–2395.
- 930 Cristofanelli, P., Bonasoni, P., 2009. Background ozone in the southern europe
931 and mediterranean area: Influence of the transport processes. *Env. Poll.* 157,
932 1399–1406.
- 933 De Meij, A., Krol, M., Dentener, F., Vignati, E., Cuvelier, C., Thunis, P., 2006.
934 The sensitivity of aerosol in europe to two different emission inventories and
935 temporal distribution of emissions. *Atmos. Chem. Phys.* 6, 42874309.
- 936 Dudhia, J., 1989. Numerical study of convection observed during the winter mon-
937 soon experiment using a mesoscale two-dimensional model. *J. Atmos. Sci.* 46
938 (20), 3077–3107, doi:10.1175/1520–0469.
- 939 Dyer, A.J., Hicks, B.B., 1970. Flux-gradient relationships in the constant flux
940 layer. *Q. J. R. Meteorol. Soc.* 96 (410), 715721, doi:10.1002/qj.49709641012.

- 941 Eder, B., Yu, S., 2006. A performance evaluation of the 2004 release of models-3
942 cmaq. *Atmos. Environ.* 40, 4811–4824, doi:10.1016/j.atmosenv.2005.08.045.
- 943 EEA, 2000. CORINE Land Cover, 2000. Technical Report. European Environ-
944 mental Agency. <http://dataservice.eea.eu.int/dataservice>, February 2007.
- 945 EEA, 2005. Air pollution by ozone in Europe in summer 2004. Technical Report.
946 3/2005, Copenhagen, Denmark. <http://reports.eea.eu.int>.
- 947 EEA, 2007. Air pollution in Europe 1999-2004. Technical Report. 2/2007, Lux-
948 embourg, Office for Official Publications of the European Communities. 79 pp.
- 949 Eisele, H., Scheel, H.E., Sladkovic, R., Trickl, T., 1999. High-resolution lidar
950 measurements of stratosphere–troposphere exchange. *J. Atmos. Sci.* 56, 319–
951 330.
- 952 EMEP, 2007. National emissions reported to the Convention on Long-range
953 Transboundary Air Pollution (LRTAP Convention). Air emission annual data
954 reporting (EMEP/MS-CW). Technical Report. European Environmental
955 Agency, The Norwegian Meteorological Institute, Oslo, Norway.
- 956 Emmerson, K.M., Evans, M.J., 2009. Comparison of tropospheric gas-phase
957 chemistry schemes for use within global models. *Atmos. Chem. Phys.* 9, 1831–
958 1845.
- 959 ESRI, 2003. Europe Highways Cartography 2003. Technical Report. GIS de ESRI
960 (ESRI España Geosistemas S.A: <http://www.esri-es.com>).
- 961 European Commission, 1996. Council Directive 96/62/EC of 27 September 1996
962 on ambient air quality assessment and management laid the foundations for
963 a common strategy to define and establish objectives for ambient air quality.
964 Technical Report 1996/62/EC, L296. *Off. J. Eur. Comm.*
- 965 European Commission, 1999. Council Directive 1999/30/EC of 22 April 1999 re-
966 lating to limit values for sulphur dioxide, nitrogen dioxide and oxides of nitro-
967 gen, particulate matter and lead in ambient air. Technical Report 1999/30/EC,
968 L 163. *Off. J. Eur. Comm.*
- 969 European Commission, 2001. Commission Decision of 17 October 2001 amend-
970 ing Annex V to Council Directive 1999/30/EC relating to limit values for sul-
971 phur dioxide, nitrogen dioxide and oxides of nitrogen, particulate matter and

- 972 lead in ambient air (Text with EEA relevance) (notified under document num-
973 ber C(2001) 3091). Technical Report 2001/744/EC, 278. Off. J. Eur. Comm.
- 974 European Commission, 2002. Directive 2002/3/EC of the European Parliament
975 and of the Council of 12 February 2002 relating to ozone in ambient air. Tech-
976 nical Report 2002/3/EC, L67. Off. J. Eur. Comm.
- 977 European Commission, 2008. Directive 2008/50/EC of the European Parliament
978 and of the Council of 21 May 2008 on ambient air quality and cleaner air for
979 Europe. Technical Report 2008/50/EC, L152. Off. J. Eur. Comm.
- 980 Folberth, G., Hauglustaine, D.A., Lathièrre, J., Brocheton, J., 2006. Interactive
981 chemistry in the laboratoire de météorologie dynamique general circulation
982 model: model description and impact analysis of biogenic hydrocarbons on
983 tropospheric chemistry. *Atmos. Chem. Phys.* 6, 2273–2319.
- 984 Gerasopoulos, E., Kouvarakis, G., Vrekoussis, M., Kanakidou, M., Mihalopou-
985 los, N., 2005. Ozone variability in the marine boundary layer of the eastern
986 mediterranean based on 7-year observations. *J. Geophys. Res.* 110, D15309.
- 987 Gery, M.W., Whitten, G.Z., Killus, J.P., Dodge, M.C., 1989. A photochemical ki-
988 netics mechanism for urban and regional scale computer modeling. *J. Geophys.*
989 *Res.* 94 (D10), 12925–12956.
- 990 Gong, S.L., 2003. A parameterization of sea-salt aerosol source func-
991 tion for sub- and super-micron particles. *J. Geophys. Res.* 17, 1097,
992 doi:10.1029/2003GB002079.
- 993 Guerova, G., Bey, I., Attié, J.L., Martin, R.V., Cui, J., Sprenger, M., 2006. Impact
994 of transatlantic transport episodes on summertime ozone in europe. *Atmos.*
995 *Chem. Phys.* 6, 2057–2072.
- 996 Hass, H., van Loon, M., Kessler, C., Stern, R., Matthijsen, J., Sauter, F., Zlatev,
997 Z., Langner, J., Foltescu, V., Schaap, M., 2003. Aerosol Modeling: Results and
998 Intercomparison form European Regional scale Modeling Systems. Technical
999 Report. EUROTRAC 2 Report, EUREKA Environmental Project, GLOREAM.
- 1000 Hauglustaine, D.A., Hourdin, F., Jourdain, L., Filiberti, M.A., Walters, S., Lamar-
1001 que, J.F., Holland, E.A., 2004. Interactive chemistry in the laboratoire de

- 1002 meteorologic dynamique general circulation model: Description and back-
1003 ground tropospheric chemistry evaluation. *J. Geophys. Res.* D4 (D04314),
1004 doi:10.1029/2003JD003,957.
- 1005 Hewitt, C.D., Griggs, D.J., 2004. Ensembles-based Predictions of Climate
1006 Changes and their Impacts. Technical Report. 1, Eos, 85.
- 1007 Hong, S.Y., Dudhia, J., Chen, S.H., 2004. A revised approach to ice microphys-
1008 ical processes for the bulk parameterization of clouds and precipitation. *Mon.*
1009 *Weather Rev.* 132 (1), 103–120, doi:10.1175/1520–0493.
- 1010 International Maritime Organization and Marine Environment Protection Com-
1011 mittee, 2001. Prevention of air pollution from ships-Sulfur monitoring 2000.
1012 Technical Report. London.
- 1013 Jacobson, M.Z., 2001. Global direct radiative forcing due to multicomponent
1014 anthropogenic and natural aerosols. *J. Geophys. Res.* 106 (D2), 1551–1568,
1015 doi:2000JD900514.
- 1016 Janjic, Z.I., 1977. Pressure gradient force and advection scheme used for forecast-
1017 ing with steep and small scale topography. *Contr. Atmos. Phys.* 50, 186–199.
- 1018 Janjic, Z.I., 1979. Forward-backward scheme modified to prevent twogrid-interval
1019 noise and its application in sigma coordinate models. *Contr. Atmos. Phys.* 52,
1020 69–84.
- 1021 Janjic, Z.I., 1984. Non-linear advection schemes and energy cascade on semi-
1022 staggered grids. *Mon. Weather Rev.* 112, 1234–1245.
- 1023 Janjic, Z.I., 1990. The step-mountain coordinate: Physical package. *Mon.*
1024 *Weather Rev.* 118, 1429–1443.
- 1025 Janjic, Z.I., 1994. The step-mountain eta coordinate model: Further developments
1026 of the convection, viscous sublayer and turbulence closure schemes. *Mon.*
1027 *Weather Rev.* 122, 927–945.
- 1028 Japar, S.M., Brachaczek, W.W., Gorse Jr., R.A., Norbeck, J.M., Pierson, W.R.,
1029 1986. The contribution of elemental carbon to the optical properties of rural
1030 atmospheric aerosols. *Atmos. Environ.* 20, 12811289.

- 1031 Jiang, W., Smyth, S., Giroux, E., Roth, H., Yin, D., 2006. Differences between
1032 cmaq fine mode particle and pm_{2.5} concentrations and their impact on model
1033 performance evaluation in the lower fraser valley. *Atmos. Environ.* 40, 4973–
1034 4985.
- 1035 Jiménez-Guerrero, P., Jorba, O., Baldasano, J.M., Gassó, S., 2008. The use of a
1036 modelling system as a tool for air quality management: Annual high-resolution
1037 simulations and evaluation. *Sci. Tot. Env.* 390, 323–340.
- 1038 Jiménez, P., Baldasano, J.M., Dabdub, D., 2003. Comparison of photochemical
1039 mechanisms for air quality modelling. *Atmos. Environ.* 37 (30), 4179–4194,
1040 doi:10.1016/S1352-2310(03)00567-3.
- 1041 Jiménez, P., Lelieveld, J., Baldasano, J.M., 2006. Multi-scale modeling
1042 of air pollutants dynamics in the northwestern mediterranean basin during
1043 a typical summertime episode. *J. Geophys. Res.* 111, (D18306), 1–21,
1044 doi:10.1029/2005JD006516.
- 1045 Kain, J.S., Fritsch, J.M., 1990. A one-dimensional entraining/detraining plume
1046 model and its application in convective parameterization. *J. Atmos. Sci.* 47
1047 (23), 27842802, doi:10.1175/1520-0469.
- 1048 Kain, J.S., Fritsch, J.M., 1993. Convective parameterization for mesoscale mod-
1049 els: The kain-fritsch scheme, the representation of cumulus convection in nu-
1050 merical models, in: Emanuel, K.A., Eds., D.R. (Eds.), *Amer. Meteor. Soc.*, pp.
1051 165–170.
- 1052 Lam, Y.F., Fu, J.S., 2009. A novel downscaling technique for the linkage of global
1053 and regional air quality modeling. *Atmos. Chem. Phys.* 9, 9169–9185.
- 1054 Larssen, S., Sluyter, R., Helmis, C., 1999. Criteria for EUROAIRNET, the EEA
1055 air quality monitoring and information network. Technical Report No. 12,
1056 <http://reports.eea.eu.int/TEC12/en>. European Environment Agency.
- 1057 Lave, L., Seskin, E.P., 1970. Air pollution and human health. *Science* 169 (3947),
1058 723–733, doi:10.1126/science.169.3947.723.
- 1059 Lelieveld, J., Berresheim, H., Borrmann, S., Crutzen, P.J., Dentener, F.J., Fis-
1060 cher, H., Feichter, J., Flatau, P.J., Heland, J., Holzinger, R., Kormann, R.,
1061 Lawrence, M.G., Levin, Z., Markowicz, K.M., Mihalopoulos, N., Minikin,
1062 A., Ramanathan, V., de Reus, M., Roelofs, G.J., Scheeren, H.A., Sciare, J.,

- 1063 Schlager, H., Schultz, M., Siegmund, P., Steil, B., Stephanou, E.G., Stier, P.,
1064 Traub, M., Warneke, C., Williams, J., Ziereis, H., 2002. Global air pollution
1065 crossroads over the mediterranean. *Science* 298, 794 – 799.
- 1066 Lipfert, F.W., 1994. *Air Pollution and Community Health - A Critical Review and*
1067 *Data Source Book*. Van Nostrand Reinhold, New York, ISBN 0-442-01444-9,
1068 576pp., 310-342.
- 1069 Li, Q., Jacob, D.J., Bey, I., Palmier, P., Duncan, B.N., Field, B.D., Mar-
1070 tin, R.V., Fiore, A.M., Yantosca, R.M., Parrish, D.D., Simmonds, P.G., Olt-
1071 mans, S.J., 2002. Transatlantic transport of pollution and its effects on sur-
1072 face ozone in europe and north america. *J. Geophys. Res.* 107 (D13), 4166,
1073 doi:10.1029/2001JD001422.
- 1074 Luecken, D.J., Phillips, S., Sarwar, G., Jang, C., 2008. Effects of using the
1075 cb05 vs. saprc99 vs. cb4 chemical mechanism on model predictions: Ozone
1076 and gas-phase photochemical precursor concentrations. *Atmos. Environ.* 42,
1077 5805–5820.
- 1078 Matthias, V., 2008. The aerosol distribution in europe derived with the community
1079 multiscale air quality (cmaq) model: comparison to near surface in situ and
1080 sunphotometer measurements. *Atmos. Chem. Phys.* 8, 5077–5097.
- 1081 Michalakes, J., Dudhia, J., Gill, D., Henderson, T., Klemp, J., Skamarock, W.,
1082 Wang, W., 2004. The weather research and forecast model: Software architec-
1083 ture and performance, in: Mozdzyński, E.G. (Ed.), To appear in proceeding of
1084 the Eleventh ECMWF Workshop on the Use of High Performance Computing
1085 in Meteorology, 2529 October 2004, Reading, U.K.. p. 117124.
- 1086 Mlawer, E.J., Taubman, S.J., Brown, P.D., Iacono, M.J., Clough, S.A., 1997. Ra-
1087 diative transfer for inhomogeneous atmosphere: Rrtm, a validated correlated-k
1088 model for the longwave. *J. Geophys. Res.* 102 (D14), 16663–16682.
- 1089 Nenes, A., Pilinis, C., Pandis, S.N., 1998. Isorropia: A new thermodynamic
1090 equilibrium model for multiphase multicomponent inorganic aerosols. *Aquatic*
1091 *Geochemistry* 4 (1), 123–152, doi:10.1023/A:1009604003981.
- 1092 Nickovic, S., Kallos, G., Papadopoulos, A., Kakaliagou, O., 2001. A model for
1093 prediction of desert dust cycle in the atmosphere. *J. Geophys. Res.* 106 (D16),
1094 18113–18129, doi:10.1029/2000JD900794.

- 1095 Noh, Y., Cheon, W.G., Hong, S.Y., Raasch, S., 2003. Improvement of the k-
1096 profile model for the planetary boundary layer based on large eddy simulation
1097 data. *Bound. Lay. Met.* 107 (2), 401–427, doi:10.1023/A:1022146015946.
- 1098 Paulson, C.A., 1970. The mathematical representation of wind speed and tem-
1099 perature profiles in the unstable atmospheric surface layer. *J. Appl. Met.* 9 (6),
1100 857–861, doi:10.1175/1520-0450.
- 1101 Pénard-Morand, C., Charpi, D., Raheison, C., Kopferschmitt, C., Caillaud, D.,
1102 Lavaud, F., Annesi-Maesano, I., 2005. Long-term exposure to background air
1103 pollution related to respiratory and allergic health in schoolchildren. *Clin. Exp.*
1104 *Allergy* 35 (10), 1279–1287, doi:10.1111/j.1365-2222.2005.02336.
- 1105 Pérez, C., Nickovic, S., Baldasano, J.M., Sicard, M., Rocadenbosch, F., Cachorro,
1106 V.E., 2006a. A long saharan dust event over the western mediterranean: Lidar,
1107 sun photometer observations, and regional dust modeling. *J. Geophys. Res.* 111
1108 (D15214), 1–16, doi:10.1029/2005JD006579.
- 1109 Pérez, C., Nickovic, S., Pejanovic, G., Baldasano, J.M., Ozsoy, E., 2006b. Interac-
1110 tive dust-radiation modeling: A step to improve weather forecasts. *J. Geophys.*
1111 *Res.* 111 (D16206), doi:10.1029/2005JD006717, 1–17.
- 1112 Piot, M., Jorba, O., Jimenez, P., Baldasano, J.M., 2008. The role of lateral bound-
1113 ary conditions and boundary layer in air quality modelling system. *Eos Trans.*
1114 *AGU* 8, H212+, Abstract A41H-0212.
- 1115 Pope, C.A.I., Ezzati, M., Dockery, D.W., 2009. Fine-particulate air pollution and
1116 life expectancy in the united states. *The New England Journ. Med.* 360, 376–
1117 386.
- 1118 Pregger, T., Friedrich, R., 2009. Effective pollutant emission heights for atmo-
1119 spheric transport modelling based on real-world information. *Environ. Poll.*
1120 157 (2), 552–560.
- 1121 Pulles, T., Kuenen, J., Pesik, J., Cadman, J., Wagner, A., 2006. EPER - The Euro-
1122 pean Pollutant Emission Register. Technical Report. <http://eper.eea.eu.int/eper>.
- 1123 Ramanathan, V., Crutzen, P.J., Kiehl, J.T., Rosenfeld, D., 2001. Aerosols,
1124 climate, and the hydrological cycle. *Science* 294 (5549), 2119–2124,
1125 doi:10.1126/science.1064034.

- 1126 Reidmiller, D.R., Fiore, A.M., Jaffe, D.A., Bergmann, D., Cuvelier, C., Dentener,
1127 F.J., N.Duncan, B., Folberth, G., Gauss, M., Gong, S., Hess, Jonson, J.E., Keat-
1128 ing, T., Lupu, A., Marmer, E., Park, R., Schultz, M.G., Shindell, D.T., Szopa,
1129 S., Vivanco, M.G., Wild, O., Zuber, A., 2009. The influence of foreign vs.
1130 north american emissions on surface ozone in the us. *Atmos. Chem. Phys.* 9,
1131 5027–5042.
- 1132 Roy, B., Mathur, R., Gilliland, A.B., Howard, S.C., 2007. A comparison of cmaq-
1133 based aerosol properties with improve, modis, and aeronet data. *J. Geophys.*
1134 *Res.* 112 (D14301), doi:10.1029/2006JD008085.
- 1135 Russell, A., Dennis, R., 2000. Narsto critical review of photochemical models
1136 and modeling. *Atmos. Environ.* 34 (12-14), 2283–2324, doi:10.1016/S1352–
1137 2310(99)00468–9.
- 1138 Sartelet, K.N., Debry, E., Fahey, K., Roustan, Y., Tombette, M., Sportisse, B.,
1139 2007. Simulation of aerosols and gas-phase species over europe with the
1140 polyphemus system: Part i. model-to-data comparison for 2001. *Atmos. En-*
1141 *viron.* 41, 6116–6131.
- 1142 Schaap, M., A.Timmermans, R.M., Roemer, M., Boersen, G.A.C., Builtjes, P.,
1143 Sauter, F., Velders, G., Beck, J., 2008. The lotos-euros model: description,
1144 validation and latest developments. *Intern. J. Environ. and Pollut.* 32, 270–290.
- 1145 Schaap, M., Gon, H.V.D., Dentener, F.J., Visschedijk, A.J.H., van Loon, M., ten
1146 Brink, H.M., Putaud, J.P., Guillaume, B., Liousse, C., Builtjes, P.J.H., 2004.
1147 Anthropogenic black carbon and fine aerosol distribution over europe. *J. Geo-*
1148 *phys. Res.* 109 (D18207), doi:10.1029/2003JD004330.
- 1149 Schell, B., Ackermann, I.J., Hass, H., Binkowski, F.S., Ebel, A., 2001. Modeling
1150 the formation of secondary organic aerosol within a comprehensive air quality
1151 model system. *J. Geophys. Res.* 106 (D22), 28275–28293, doi:2001JD000384.
- 1152 Schmidt, H., Derognat, C., Vautard, R., Beekmann, M., 2001. A comparison of
1153 simulated and observed ozone mixing ratios for the summer of 1998 in western
1154 europe. *Atmos. Environ.* 6, 6227–6297.
- 1155 Seinfeld, J.H., Pandis, S.N., 1998. *Atmospheric Chemistry and Physics.* John
1156 Wiley & Sons, New York, Chichester, Weinheim.

- 1157 Simpson, D.W., Yttri, K., Klimont, Z., Caseiro, A., Gelencser, A., Pio, C.,
1158 Puxbaum, H., Legrand, M.R., 2007. Modelling carbonaceous aerosol over eu-
1159 rope: analysis of the carbasol and emep ec/oc campaigns. *J. Geophys. Res.* 112
1160 (D23S19), doi: 10.1029/2006JD0008158.
- 1161 Simpson, D., Fagerli, H., Jonson, J., Tsyro, S., Wind, P., Tuovinen, J., 2003.
1162 Transboundary acidification and eutrophication and ground level ozone in Eu-
1163 rope. Technical Report. EMEP Status Report 1/03, Part I: Unified EMEP model
1164 description. The Norwegian Meteorological Institute, Oslo, Norway.
- 1165 Skamarock, W.C., Klemp, J.B., 2008. A time-split nonhydrostatic atmospheric
1166 model for weather research and forecasting applications. *J. Comput. Phys.* 227
1167 (7), 3465–3485, doi:10.1016/j.jcp.2007.01.037.
- 1168 Song, C.K., Byun, D.W., Pierce, R.B., Alsaadi, J.A., Schaack, T.K., Vukovich,
1169 F., 2008. Downscale linkage of global model output for regional chemical
1170 transport modeling: Method and general performance. *J. Geophys. Res.* 113,
1171 D08308, doi:10.1029/JD008951.
- 1172 Stern, R., Builtjes, P., Schaap, M., Timmermans, R., Vautard, R., Hodzic,
1173 A., Memmesheimer, M., Feldmann, H., Renner, E., Wolke, R., Ker-
1174 schbaumer, A., 2008. A model inter-comparison study focussing on
1175 episodes with elevated pm₁₀ concentrations. *Atmos. Environ.* 42, 4567–4588,
1176 doi:10.1016/j.atmosenv.2008.01.068.
- 1177 Szopa, S., Foret, G., Menut, L., Cozic, A., 2009. Impact of large scale circulation
1178 on european summer surface ozone and consequences for modelling forecast.
1179 *Atmos. Environ.* 43, 1189–1195.
- 1180 Tang, Y., Carmichael, G.R., Thongboonchoo, N., Chai, T., Horowitz, L.W.,
1181 Pierce, R.B., Al-Saadi, J.A., Pfister, G., Vukovich, J.M., Avery, M.A., Sachse,
1182 G.W., Ryerson, T.B., Holloway, J.S., Atlas, E.L., Flocke, F.M., Weber, R.J.,
1183 Huey, L.G., Dibb, J.E., Streets, D.G., Brune, W.H., 2007. Influence of lateral
1184 and top boundary conditions on regional air quality prediction: A multiscale
1185 study coupling regional and global chemical transport models. *J. Geophys.*
1186 *Res.* 112, D10S18, 2083–2097, doi: 10.1029/2006JD007515.
- 1187 Tang, Y., Lee, P., Tsidulko, M., Huang, H.C., McQueen, J.T., DiMego, G.J., Em-
1188 mons, L.K., Pierce, R.B., Lin, H.M., Kang, D., Tong, D., Yu, S.C., Mathur, R.,
1189 Pleim, J.E., Otte, T.L., Pouliot, G., Young, J.O., Schere, K.L., Davidson, P.M.,

- 1190 2008. The impact of chemical lateral boundary conditions on cmaq predictions
1191 of tropospheric ozone over the continental united states. *Environ. Fluid Mech.*
1192 9, (1), 43–58, doi:10.1007/s10652-008-9092-5.
- 1193 Tarrasón, L., Benedictow, A., Fagerli, H., Jonson, J., Klein, H., van Loon, M.,
1194 Simpson, D., Tsyro, S., Vestreng, V., Wind, P., 2005. Transboundary Acid-
1195 ification, Eutrophication and Ground Level Ozone in Europe in 2003. EMEP
1196 Status Report 1/05. Technical Report. EMEP. The Norwegian Meteorological
1197 Institute, Oslo, Norway.
- 1198 Tarrasón, L., Fagerli, H., Jonson, J.E., Simpson, D., Benedictow, A., Klein, H.,
1199 Vestreng, V., 2007. Transboundary Acidification, Eutrophication and Ground
1200 Level Ozone in Europe in 2005. Technical Report. EMEP Status Report 1/07.
1201 The Norwegian Meteorological Institute, Oslo, Norway.
- 1202 Tarrasón, L., Fagerli, H., Klein, H., Simpson, D., Benedictow, A., Vestreng,
1203 V., Rigler, E., Emberson, L., Posch, M., Spranger, T., 2006. Transboundary
1204 Acidification, Eutrophication and Ground Level Ozone in Europe from 1990 to
1205 2004. Technical Report. EMEP Status Report 1/06: to support the review of the
1206 Gothenburg Protocol. The Norwegian Meteorological Institute, Oslo, Norway.
- 1207 Thibodeau, L.A., Reed, R.B., Bishop, Y.M.M., Kammerman, L.A., 1980. Air
1208 pollution and human health: A review and reanalysis. *Environ. Health Perspec.*
1209 34, 165–183.
- 1210 Torseth, K., Hov, O., 2003. The EMEP monitoring strategy 2004-2009. Technical
1211 Report 9/2003. EMEP/CCC.
- 1212 Tsyro, S.G., 2005. To what extent can aerosol water explain the discrepancy
1213 between model calculated and gravimetric PM_{10} and $PM_{2.5}$. *Atmos. Chem.*
1214 *Phys.* 5, 515–532.
- 1215 Tsyro, S., Simpson, D., Tarrasón, L., Klimont, Z., Kupiainen, K., Pio, C., Yttri,
1216 K.E., 2007. Modeling of elemental carbon over europe. *J. Geophys. Res.* 112,
1217 D23S19.
- 1218 U.S. EPA, 1984. Interim procedures for evaluating air quality models (revised).
1219 Technical Report. EPA-450/4-91-013. U.S. Environmental Protection Agency,
1220 Office of Air Quality Planning and Standards: Research Triangle Park, NC.

- 1221 U.S. EPA, 1991. Guideline for regulatory application of the urban airshed model.
1222 Technical Report. EPA-450/4-91-013. U.S. Environmental Protection Agency,
1223 Office of Air Quality Planning and Standards: Research Triangle Park, NC.
- 1224 U.S. EPA, 2007. Guidance on the Use of Models and Other Analyses for Demon-
1225 strating Attainment of Air Quality Goals for Ozone, PM_{2.5}, and Regional
1226 Haze. Technical Report. EPA-454/B-07-002. U.S. Environmental Protection
1227 Agency, Office of Air Quality Planning and Standards: Research Triangle Park,
1228 NC.
- 1229 van Loon, M., Roemer, M.G.M., Builtjes, P.J.H., Bessagnet, B., Rouïll, L., Chris-
1230 tensen, J., Brandt, J., Fagerli, H., Tarrasón, L., Rodgers, I., 2004. Model inter-
1231 comparison In the framework of the review of the Unified EMEP model. TNO
1232 Report. Technical Report. R2004/282. 53 pp.
- 1233 van Loon, M., Vautard, R., Schaap, M., Bergstrom, R., Bessagnet, B., Brandt,
1234 J., Builtjes, P., Christensen, J., Cuvelier, C., Graff, A., Jonson, J.E., Krol, M.,
1235 Langner, J., Roberts, P., Rouïl, L., Stern, R., Tarrasón, L., Thunis, P., Vignati,
1236 E., White, L., Wind, P., 2007. Evaluation of long-term ozone simulations from
1237 seven regional air quality models and their ensemble. *Atmos. Environ.* 41,
1238 2083–2097, doi:10.1016/j.atmosenv.2006.10.073.
- 1239 Vautard, R., Bessagnet, B., Chin, M., Menut, L., 2005a. On the contribution of
1240 natural aeolian sources to particulate matter concentrations in europe: Testing
1241 hypotheses with a modelling approach. *Atmos. Environ.* 39 (18), 3291–3303,
1242 doi:10.1016/j.atmosenv.2005.01.051.
- 1243 Vautard, R., Honoré, C., Beekmann, M., Rouïl, L., 2005b. Simulation of ozone
1244 during the august 2003 heat wave and emission control scenarios. *Atmos. En-
1245 viron.* 39 (16), 2957–2967, doi:10.1016/j.atmosenv.2005.01.039.
- 1246 Vautard, R., Schaap, M., Bergström, R., Bessagnet, B., Brandt, J., Builtjes, P.J.H.,
1247 Christensen, J.H., Cuvelier, C., Foltescu, V., Graff, A., Kerschbaumer, A., Krol,
1248 M., Roberts, P., Rouïl, L., Stern, R., Tarrason, L., Thunis, P., Vignati, E., Wind,
1249 P., 2009. Skill and uncertainty of a regional air quality model ensemble. *Atmos.
1250 Environ.* 43, 4822–4832, doi:10.1016/j.atmosenv.2008.09.083.
- 1251 Webb, E.K., 1970. Profile relationships: The log-linear range, and ex-
1252 tension to strong stability. *Q. J. R. Meteorol. Soc.* 96 (407), 67–90,
1253 doi:10.1002/qj.49709640708.

- 1254 Weil, J.C., Sykes, R.I., Venkatram, A., 1992. Evaluating air-quality models: re-
1255 view and outlook. *J. Appl. Met.* 31, 1121–1145.
- 1256 Wesely, M.L., Hicks, B., 2000. A review of the current status of knowledge on
1257 dry deposition. *Atmos. Environ.* 34, 2261–2282.
- 1258 Wyat Appel, K., Bhave, P.V., Gilliland, A.B., Sarwar, G., Roselle, S.J., 2008.
1259 Evaluation of the community multiscale air quality (cmaq) model version 4.5:
1260 Sensitivities impacting model performance; part ii particulate matter. *Atmos.*
1261 *Environ.* 42 (24), 6057–6066, doi:10.1016/j.atmosenv.2008.03.036.
- 1262 Wyat Appel, K., Gilliland, A., Sarwar, G., Gilliam, R.C., 2007. Evaluation of the
1263 community multiscale air quality (cmaq) model version 4.5: Uncertainties and
1264 sensitivities impacting model performance: Part i - ozone. *Atmos. Environ.* 41
1265 (40), 9603–9613.
- 1266 Yarwood, G., Rao, S., Yocke, M., Whitten, G.Z., 2005. Updates to the Carbon
1267 Bond chemical mechanism: CB05. Technical Report RT-0400675, December,
1268 8. Final Report to the US EPA.
- 1269 Yttri, K.E., Aas, W., Forster, C., Torseth, K., Tsyro, S., Tarrasón, L., Simpson,
1270 D., Vestreng, V., Lazaridis, M., Kopanakis, I., Aleksandropoulou, V., Gehrig,
1271 R., Adams, M., Woodfield, M., Putaud, J., Schultz, M., 2006. Transboundary
1272 particulate matter in Europe. Technical Report. EMEP Status Report 4/06. The
1273 Norwegian Meteorological Institute, Oslo, Norway.
- 1274 Yttri, K.E., Hanssen, J.E., Tsyro, S., Lazaridis, M., Facchini, M.C., Jennings,
1275 S.G., 2005. Transboundary particulate matter in Europe. Technical Report.
1276 EMEP Status Report 4/05. The Norwegian Meteorological Institute, Oslo, Nor-
1277 way.
- 1278 Yu, S., Eder, B., Dennis, R., Chu, S., Schwartz, S., 2006. New unbiased symmetric
1279 metrics for evaluation of air quality models. *Atmos. Sci. Lett.* 7, 26–34.
- 1280 Zhang, K., Knipping, E., Wexler, A., Bhave, P., Tonnesen, G., 2005. Size distri-
1281 bution of sea-salt emissions as a function of relative humidity. *Atmos. Environ.*
1282 39, 3373–3379.
- 1283 Zhang, Y., Liu, P., Pun, B., Seigneur, C., 2006. A comprehensive performance
1284 evaluation of mm5-cmaq for the summer 1999 southern oxidants study episode,

REFERENCES

47

- 1285 part iii: Diagnostic and mechanistic evaluations. *Atmos. Environ.* 40, 4856–
1286 4873, doi:10.1016/j.atmosenv.2005.12.046.

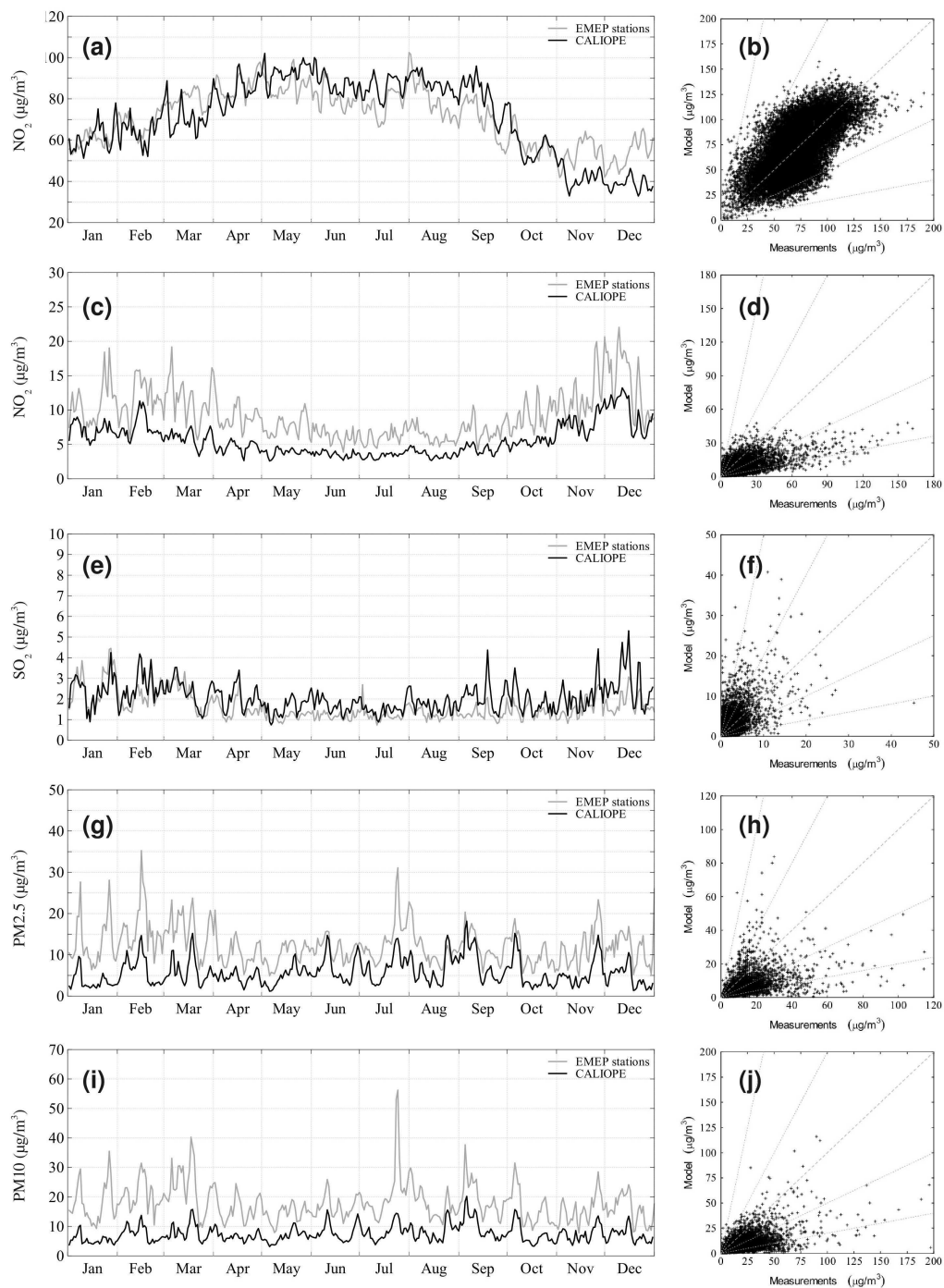


Figure 3: Modeled (black lines) and measured (grey lines) time series of daily mean concentrations (left) and scatter plots (right) for O_3 , NO_2 , SO_2 , $\text{PM}_{2.5}$ and PM_{10} , respectively, at the EMEP stations. The scatter plots include the 1:1, 1:2, 2:1, 1:5 and 5:1 reference lines.

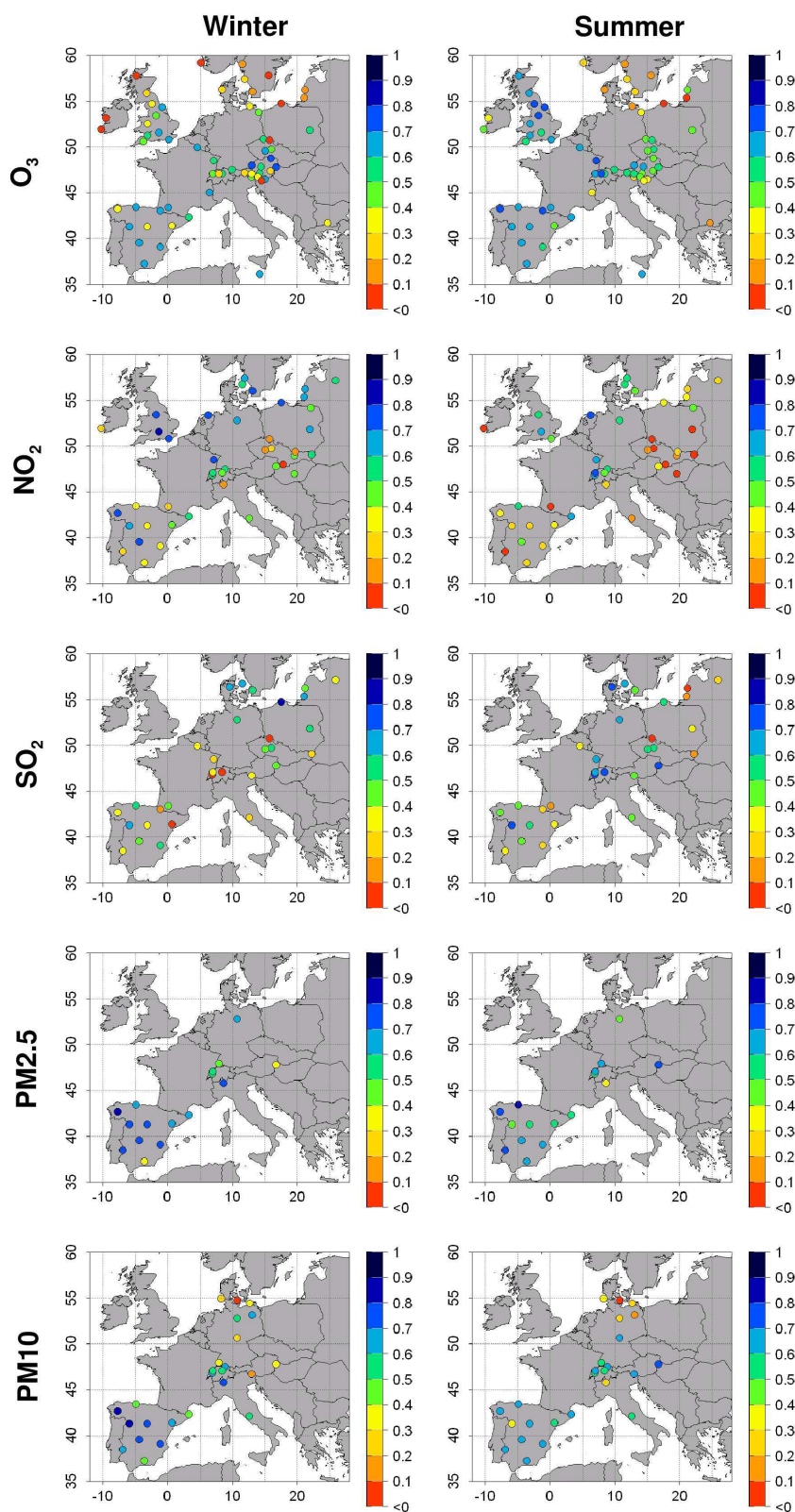


Figure 4: Spatial distribution of the correlation coefficient at all stations for O₃, NO₂, SO₂, PM_{2.5} and PM₁₀. The two columns represent the winter and summer seasons for 2004, respectively.

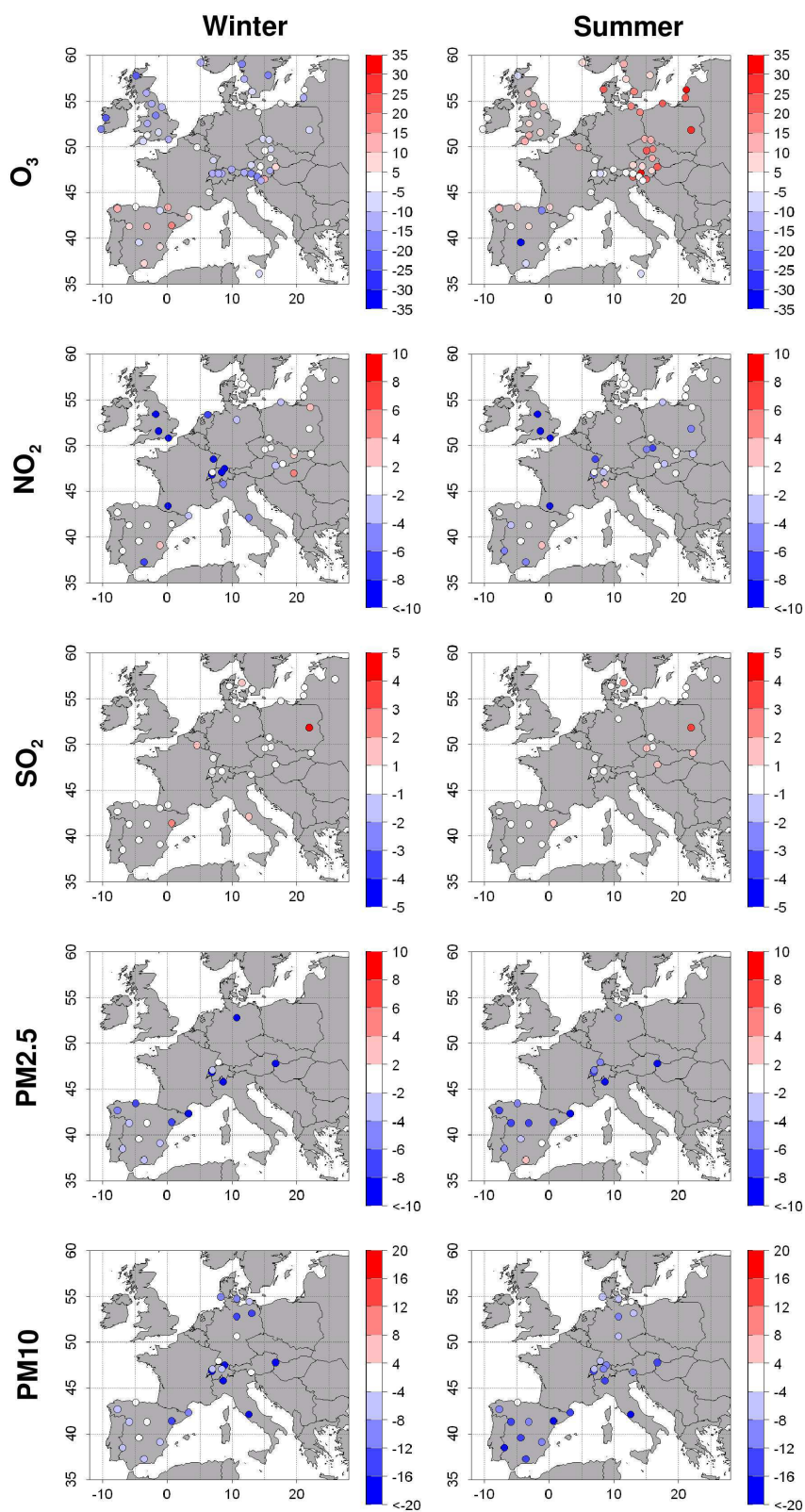


Figure 5: Spatial distribution of mean bias at all stations for O₃, NO₂, SO₂, PM_{2.5} and PM₁₀ (in $\mu\text{g m}^{-3}$). The two columns represent the winter and summer seasons for 2004, respectively.

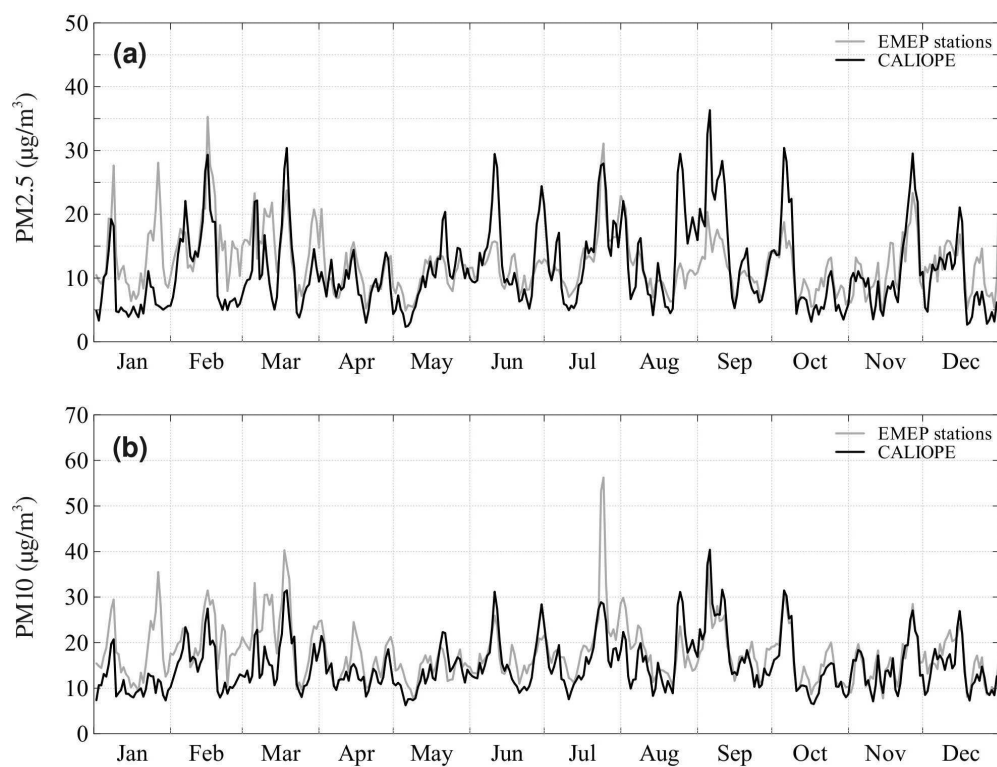


Figure 6: Modeled (black lines) and measured (grey lines) time series of daily mean concentrations for PM_{2.5} (top) and PM₁₀ (bottom), multiplied by a correction factor of 2 at the EMEP stations.

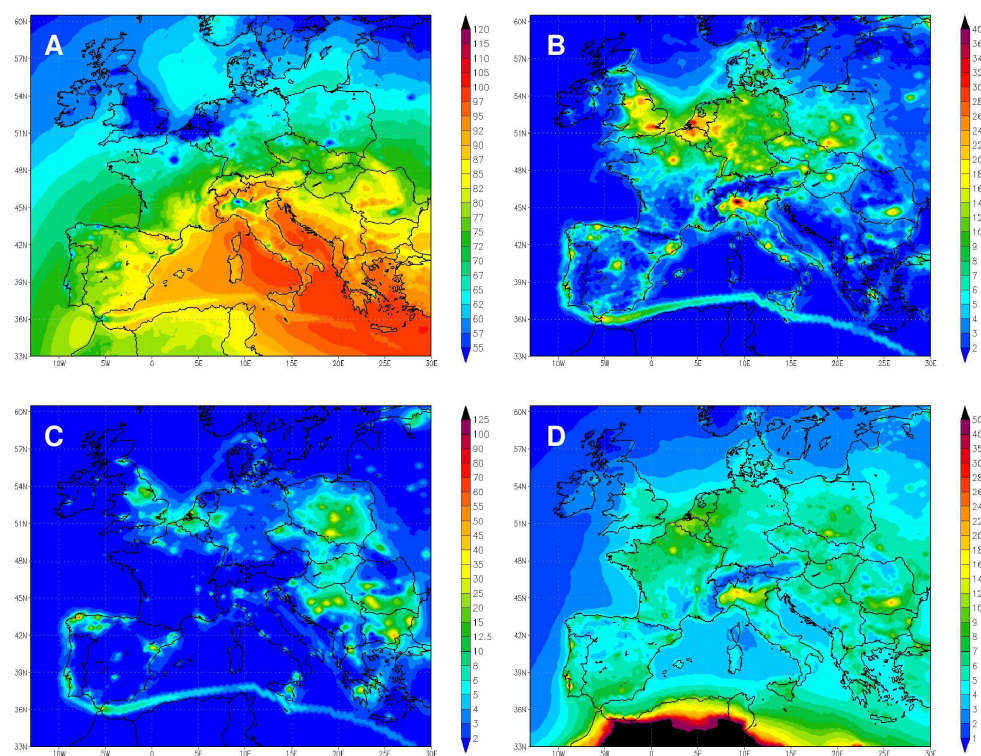


Figure 7: Simulated annual average concentrations ($\mu\text{g m}^{-3}$) of (a) O₃, (b) NO₂, (c) SO₂, (d) PM_{2.5} at ground level modeled with the CALIOPE-EU air quality modeling system for Europe with a $12 \text{ km} \times 12 \text{ km}$ spatial resolution in 2004.

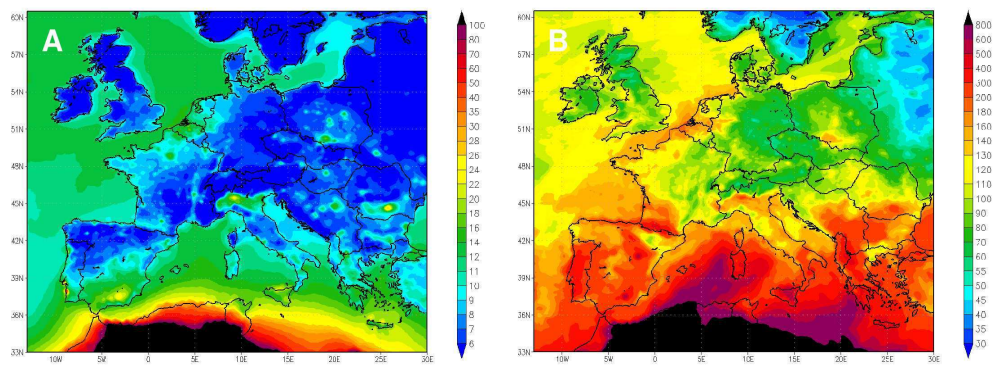


Figure 8: Simulated annual (a) average and (b) maximum concentrations for PM10 in $\mu\text{g m}^{-3}$ in 2004.